



1 **Characteristics of Water Masses in the Atlantic Ocean based**  
2 **on GLODAPv2 data**

3 Mian Liu<sup>1</sup>, Toste Tanhua<sup>1</sup>

4 <sup>1</sup>Marine Biogeochemistry, Chemical Oceanography, GEOMAR Helmholtz Centre for Ocean Research Kiel,  
5 Düsternbrooker Weg 20, 24105 Kiel, Germany

6 *Correspondence to:* T. Tanhua (ttanhua@geomar.de)

7



8 **Abstract:** The characteristics of the main water masses in the Atlantic Ocean are investigated and defined as  
9 Source Water Types (SWTs) from their formation area by six key properties based on the GLODAPv2  
10 observational data. These include both conservative (potential temperature and salinity) and non-conservative  
11 (oxygen, silicate, phosphate and nitrate) variables. For this we divided the Atlantic Ocean into four vertical  
12 layers by distinct potential densities in the shallow and intermediate water column, and additionally by  
13 concentration of silicate in the deep waters. The SWTs in the upper/central water layer originates from  
14 subduction during winter and are defined as central waters, formed in four distinct areas; East North Atlantic  
15 Central water (ENACW), West North Atlantic Central Water (WNACW), East South Atlantic Central Water  
16 (ESACW) and West South Atlantic Central Water (WSACW). Below the upper/central layer the intermediate  
17 layer consist of three main SWTs; Antarctic Intermediate Water (AAIW), Subarctic Intermediate Water (SAIW)  
18 and Mediterranean Overflow Water (MOW). The North Atlantic Deep Water (NADW) is the dominating SWT  
19 in the deep and overflow layer, and is divided into upper and lower NADW based on the different origins and  
20 properties. The origin of both the upper and lower NADW is the Labrador Sea Water (LSW), the Iceland-  
21 Scotland Overflow Water (ISOW) and Denmark Strait Overflow Water (DSOW). Antarctic Bottom Water  
22 (AABW) is the only natural SWT in the bottom layer and this SWT is redefined as North East Atlantic Bottom  
23 Water (NEABW) in the north of equator due to the change of key properties, especial silicate. Similar with  
24 NADW, two additional SWTs, Circumpolar Deep Water (CDW) and Weddell Sea Bottom Water (WSBW), are  
25 defined in the Weddell Sea in order to understand the origin of AABW. The definition of water masses in  
26 biogeochemical space is useful for, in particular, chemical and biological oceanography to understand the origin  
27 and mixing history of water samples.

28

29 **Key Words:** Water Mass, Source Water Types, GLODAP, Atlantic Ocean

30



## 31 1. Introduction

32 Properties of water in the ocean are, obviously, not uniformly distributed so that different regions and depths (or  
33 densities) are characterized by different properties. Bodies of water with similar properties often share a common  
34 formation history and are referred to as water masses, or, more generally, sea water types. Understanding of the  
35 distribution and variation of water masses play an important role in several disciplines of oceanography, for  
36 instance while investigating the thermohaline circulation of the world ocean or predicting climate changes (e.g.  
37 Haine and Hall, 2002; Tomczak, 1999). Particularly important is the concept of water masses for biogeochemical  
38 and biological applications where the transformation of properties over time can be successfully viewed in the  
39 water mass frame-work. For instance, the formation of Denmark Strait Overflow water in the Denmark Strait  
40 could be described using mixing of a large number of water masses from the Arctic Ocean and the Nordic Seas  
41 (Tanhua et al., 2005). In a more recent work, Garcia-Ibanez et al. (2015) considered 14 water masses combined  
42 with velocity fields to estimate transport of water mass, and thus chemical constituents, in the north Atlantic.  
43 Similarly, Jullion et al. (2017) used water mass analysis in the Mediterranean Sea to better understand the  
44 dynamics of dissolved Barium. Also, Wüst and Defant (1936) illustrated the stratification and circulation of  
45 water masses in the Atlantic Ocean based on the observational data from Meteor Cruise 1925-1927. Based on  
46 research during last few decades, Tomczak (1999) summarized the history of the water mass research and  
47 provided an outlook for the evolution of water mass research. In this paper we use the concepts and definitions  
48 of water masses as given by Tomczak (1999).

49 The definition of a water mass is a body of water that originates in a particular area of the ocean with a common  
50 formation history. Water masses share common properties such as temperature, salinity and biogeochemical  
51 variables that are distinct from surrounding bodies of water (e.g. Helland-Hansen, 1916; Montgomery, 1958) and  
52 have a measurable extent both in the vertical and horizontal, and thus a quantifiable volume. Since water masses  
53 are surrounded by other water masses there will be mixing (both along and across density surfaces) between the  
54 water masses, so that away from the formation regions one tend to find mixtures of water masses with different  
55 properties compared to the ones in the formation area. Early work by Schaffer and JACOBSEN (1927) and  
56 Defant (1929) illustrated the application of T-S relationship in the oceanography. This concept has been  
57 redefined over time and in Emery and Meincke (1986), for instance, the water masses were divided into upper,  
58 intermediate and deep/abyssal layers including the depth to the T-S relationship. With the development of  
59 observational capacities for a range of variables, definition of water masses is not only limited by the T-S-P  
60 relationship. New physical and chemical parameters, both conservative and non-conservative, are added in the  
61 water mass concept e.g. (Tomczak, 1981; Tomczak and Large, 1989). These additional variables exhibit  
62 different importance in defining a water masses but are complementary to each other and provide a more solid  
63 basis for the water mass definition.

64 The ocean is thus composed a large number of water masses, these are however not simply piled up in the ocean  
65 like bricks. In fact, there are no clear boundaries between them. Or, in other words, there is a gradual and mixed  
66 process between water masses (Castro et al., 1998). As a direct result another concept was introduced: Source  
67 Water Types (SWTs). SWTs describe the original properties of water masses in their formation area, and can  
68 thus be considered as the original form of water masses (Tomczak, 1999).

69 It is important to realize that while water masses have a defined volume and extent, a water type is only a  
70 mathematical definition that does not have a physical extent. A SWT is defined based on a number of properties



71 and their variance, or standard deviation (Tomczak, 1999). Knowledge of the properties of the SWTs is essential  
72 in labeling water masses, tracking their spreading and mixing progresses. Accurate definition and  
73 characterization of SWTs is an essential step for performing any water mass mixing analysis, such as the  
74 Optimum Multi-parameter (OMP) analysis (Tomczak and Large, 1989). In practice though, defining properties  
75 of source water types and water masses is often a difficult and time-consuming part of water mass analysis,  
76 particularly when analyzing data from a region distant from the water mass formation regions. In order to  
77 facilitate water mass analysis we use the Atlantic data from the data product GLODAPv2 (Lauvset et al., 2016)  
78 to identify and define source water types for the most prominent water masses in the Atlantic Ocean based on 6  
79 commonly measured physical and biogeochemical variables. The aim of this work is to facilitate water mass  
80 analysis and in particular we aim at supporting biogeochemical and biological oceanographic work in a broad  
81 sense. We realize that we define the SWTs in a static sense, i.e. we assume that they do not change with time,  
82 and that our analysis is relatively coarse in that we do not consider subtle differences between closely related  
83 SWTs but rather paint the picture with a rather broad brush. Studies looking at temporal variability of water  
84 masses, or water mass formation processes in detail, for instance, may find this study useful but will certainly  
85 want to use a more granular approach to water mass analysis in their particular area.

86 In a companion paper (Liu and Tanhua, 2018) we will use the here defined Atlantic Ocean SWTs to estimate the  
87 distribution of the water masses in the Atlantic Ocean based on the GLODAPv2 data.

88





## 89 2. Data and Methods

90 In this study we use six key variables to define source water types (SWTs) in Atlantic Ocean, including two  
91 conservative variables, potential temperature ( $\theta$ ) and salinity (S), and four non-conservative variables, silicate,  
92 oxygen, phosphate and nitrate. We utilize the GLODAPv2 data product (Lauvset et al., 2016) to quantify the  
93 properties and related standard deviation of these variables for Atlantic Ocean SWTs. The GLODAPv2 data  
94 product is a compilation of interior ocean carbon relevant data from ship-based observations and includes data  
95 on oxygen and nutrients. The data in the GLODAPv2 product has passed both a primary quality control (aiming  
96 at precision of the data) and a secondary data quality control (aiming at the accuracy of the data). The data  
97 product that we use in this work thus uses adjusted values to correct for any biases in data. The methodologies  
98 for the QC processes in GLODAPv2 are similar to those used for the CARINA data product and are described in  
99 detail in (Key et al., 2010). Through these QC routines, the GLODAPv2 product is unique in its internal  
100 consistency, and is thus an ideal product to use for this work aiming at definitions of major water masses and  
101 source water types in the Atlantic Ocean. Armed with the internally consistent data in GLODAPv2, we utilize  
102 previously published studies on water masses and their formation areas to define areas and depth / density ranges  
103 that can be considered to be representative samples of a SWT. As a second step we characterize the SWT in a 6  
104 parameter space by quantifying the concentrations of these variables and use the standard deviation as a measure  
105 of the variability of each SWT and variable combination.

## 106 3 Source Water Types (SWTs) in the Atlantic Ocean

107 In line with the results from Emery and Meincke (1986) and from our interpretation of the observational data  
108 from GLODAPv2, we consider that the water masses in the Atlantic Ocean are distributed in four main vertical  
109 layers (Figure 1) roughly separated by surfaces of equal density. Potential density is the main basis to divide the  
110 shallow layers whereas for the deep and bottom layers the concentration of silicate is additionally used to  
111 distinguish these layers. In this concept we do not consider the mixed layer as its properties tend to be strongly  
112 variable on seasonal time-scales so that other methods to characterize the water masses is needed, mostly based  
113 on geographic region. The Upper Layer is the shallowest layer (i.e. lowest density) under consideration and is  
114 located within upper 500-1000m of the water column but below the mixed layer. The Intermediate Layer is  
115 located between ~1000 to 1500/2000m, below the Upper Layer. The Deep and Overflow layer occupies the layer  
116 roughly between 2000-4000m of the Atlantic Ocean. The Bottom Layer is the deepest layer, mostly located  
117 below 4000m, and is often characterized by high silicate concentrations. In this section we will identify key  
118 SWTs in each of the four layers. Table 1 lists the four layers and the water masses that we consider in this study.  
119 The table also lists the selection criteria that we used to define a Source Water Type in pressure, potential  
120 temperature or density space, for some SWTs, key properties such as salinity, oxygen or silicate are also  
121 necessary, in order to characterize the biogeochemical properties as well.

122 During our narrative of each SWT we will display four figures that will guide us to a more intuitive  
123 understanding of the SWTs: (a) maps of all GLODAPv2 station locations marked as light gray dots where  
124 stations within the area of formation that we consider are marked in red and stations with any samples within the  
125 desired properties as defined by Table 1 in blue, (b) the T-S relationship with the same color coding, (c) depth  
126 profiles of the 6 variables under consideration (same color coding), and (d) bar plots of the distribution of the  
127 samples within the criteria for a SWT. In the bar plot we have added a Gaussian curve to the distribution derived



128 from the average and standard deviation of the distribution (the amplitude of the curve defined as 2/3 of the  
129 highest bar). The plots of properties vs pressure provides an intuitive understanding of each STW compared to  
130 others in the same region. The properties distribution and the Gaussian curve will help us to visually determine  
131 and confirm the SWT property values and associated standard deviation.

### 132 3.1 The Upper Layer, Central Waters

133 The Upper Layer is occupied by four SWTs called central waters that are known to be formed by subducted into  
134 the thermocline (Sprintall and Tomczak, 1993; Tomczak and Godfrey, 2013) into the interior of the ocean  
135 (Pollard et al., 1996). Figure 2 illustrate a schematic of the main currents in this layer and the main formation  
136 regions of the central waters in the Atlantic Ocean. Water masses or SWTs in this layer can be easily recognized  
137 by their linear T-S relationship (Pollard et al., 1996; Stramma and England, 1999). In this study, we define upper  
138 layer water masses to be located above potential density isoline of  $27.0 \text{ kg/m}^3$  (see Fig 3.0), but below the mixed  
139 layer. The formation and transport of the Central Water is influenced by the currents in the shallow layer and  
140 finally forms a relative distinct body of water in both the horizontal and vertical. Mode Waters, on the other  
141 hand, are considered as the precursor or the prototype of the central waters (Alvarez et al., 2014; Cianca et al.,  
142 2009). In this study we will refer to Mode Waters in the description in defining or formation of the central waters  
143 but do not relate to their details.

#### 144 3.1.1 Eastern North Atlantic Central Water (ENACW)

145 The main water mass in the upper layer of the region east of the Mid Atlantic Ridge (MAR) is the East North  
146 Atlantic Central Water (ENACW) (Harvey, 1982). This water mass is formed during winter and gets subducted  
147 in the seas west of Iberian Peninsula. In addition, one component of the Subpolar Mode Water (SPMW) is  
148 carried by the south branch of North Atlantic Current (Figure 3a) and mixed in ESAW contributing to the  
149 properties of this water mass (McCartney and Talley, 1982) so that ENACW shows a typical linear T-S  
150 relationship (Pollard et al., 1996). ENACW advects in the general southern direction along the south branch of  
151 the North Atlantic Current (Arhan, 1990), passes northwest Africa, and then turns southwest into Canary basin.  
152 In the vertical scale, ENACW occupies at the upper ~500m with a relative low salinity, while SAIW is often  
153 occupying the water column below ENACW, often with contribution of MOW from the east in the intermediate  
154 depth (Garcia-Ibanez et al., 2015; Pollard et al., 1996; Pollard and Pu, 1985; Prieto et al., 2015). This  
155 stratification can also be clearly seen in the salinity/depth plot of Figure 3c where the MOW is primarily  
156 characterized by high salinity (see also Figure 9c and description of MOW ).

157 In our analysis, we follow the analysis of Pollard et al. (1996) and choose latitude between 39 and 48 °N and  
158 between 15 and 25 °E of longitude (east of Mid-Atlantic-Ridge) as the formation area of ENACW (Figure 3a).  
159 Based on the work of (Pollard and Pu, 1985) we choose potential density,  $\sigma_\theta = 26.50 \text{ kg/m}^3$  as higher boundary  
160 and  $\sigma_\theta = 27.30 \text{ kg/m}^3$  as the lower boundary to define ENACW in our analysis.

161 In Figure 3b, we can see clearly the linear T-S distribution of this water masses, consistent with Pollard et al.  
162 (1996) and the definition of ENACW<sub>12</sub> in Garcia-Ibanez et al. (2015). In Garcia-Ibanez et al. (2015), there is  
163 another definition ENACW<sub>16</sub>, but water samples show a discrete distribution warmer than 16 °C by GLODAPv2  
164 data set in this region, so also samples with potential temperature below 16 °C are selected in this study. As



165 shown in Figure 3c, ENACW dominates the upper 500m depth. The main character of ENACW is the large  
166 potential temperature and salinity ranges and low nutrients (especially low in silicate).

### 167 3.1.2 Western North Atlantic Central Water (WNACW)

168 Western North Atlantic Central Water (WNACW) is another SWT formed during winter through subduction  
169 (McCartney and Talley, 1982; Worthington, 1959). WNACW is formed at the south flank of the Gulf Stream  
170 (Klein and Hogg, 1996) and is in some literatures referred to as 18 ° water since a potential temperature of  
171 around 18 °C and salinity around 36.5 are standard features of this SWT (Talley and Raymer, 1982). In general,  
172 ocean water in the Northeast Atlantic has higher salinity than in the Northwest Atlantic due to the stronger  
173 winter convection (Pollard and Pu, 1985) and input of MOW (Pollard et al., 1996; Prieto et al., 2015). However,  
174 for the central waters, we find the opposite. WNACW has a significantly higher salinity than ENACW by 0.9  
175 PSU units. This is due to a number of reasons, such as different latitudes of formation; WNACW is formed in  
176 lower latitude than ENACW so that surface water with higher salinity subducts during winter convection to form  
177 WNACW.

178 In this study, we follow McCartney and Talley (1982) and choose the region 24-37°N, 50-70°W as the formation  
179 area and pressures less than 1000 m. By defining the depth of this SWT water samples show a discrete T-S  
180 distribution with potential densities lower than 26.30 or larger than 26.60 kg/m<sup>3</sup>. Besides the potential density  
181 constraint, we added the constraint that concentrations of phosphate have to be lower than 0.3 and silicate lower  
182 than 3 μmol kg<sup>-1</sup>.

183 The properties of WNACW are shown in Figure 4. Besides the linear T-S relationship, a feature of all central  
184 waters, another feature of this water mass is, as the alternative name suggests, a potential temperature around 18  
185 °C. This is the warmest of the four STWs in the Atlantic Ocean since it has the lowest latitude of formation and  
186 is influenced by the high salinity Gulf Stream during formation. Low nutrients, including silicate, phosphate and  
187 nitrate are other features compared to other central waters that generally are low in nutrients compared to deeper  
188 water masses

### 189 3.1.3 Western South Atlantic Central Water (WSACW)

190 Western South Atlantic Central Water (WSACW) is located in the starting point that central water is transported  
191 to the north during the Meridional Overturning Circulation (Kuhlbrodt et al., 2007). For this reason, the  
192 importance of WSACW is clear. The WSACW is formed with little directly influence from other central water  
193 masses (Stramma and England, 1999), while the origin of other central water masses (e.g. ESACW or ENACW)  
194 can, to some extent at least, be traced back to WSACW (Peterson and Stramma, 1991). This water mass is a  
195 product of three mode waters mixed together: the Brazil current brings Salinity Maximum Water (SMW) and  
196 Subtropical Mode Water (STMW) from the north, while the Falkland Current brings Subarctic Mode Water  
197 (SAMW) from the south (Alvarez et al., 2014). Here we follow the work of Stramma and England (1999) and  
198 Alvarez et al. (2014) that choose the meeting region of these two currents (25-60°W, 30-45°S) as the formation  
199 region of WSACW. We choose potential density ( $\sigma_\theta$ ) between 26.0 and 27.0 kg/m<sup>3</sup> and salinity higher than 34.5  
200 for defining WSACW. In addition to the physical properties we used the requirement of silicate concentrations  
201 lower than 10 μmol kg<sup>-1</sup> and oxygen concentrations lower than 230 μmol kg<sup>-1</sup> to define this SWT.



202 The temperature distribution in this region indicates another peak in the abundance (histogram) for potential  
203 densities higher than  $27.0 \text{ kg m}^{-3}$ , indicating that the boundary between WSACW and AAIW is at  $\sigma_{\theta} = 27.0 \text{ kg}$   
204  $\text{m}^{-3}$  in this region. The hydrochemical properties of WSACW are shown in Figure 5. Similar to other central  
205 waters, WSACW shows a linear T-S relationship with large T and S ranges and low concentration of nutrients,  
206 especially low silicate.

### 207 3.1.4 Eastern South Atlantic Central Water (ESACW)

208 The other formation area of SACW in the eastern South Atlantic Ocean is located in area southwest of South  
209 Africa. In this region the Agulhas Current brings water from the Indian Ocean (Deruijter, 1982; Lutjeharms and  
210 van Ballegooyen, 1988) that meets and mixes with the South Atlantic Current (Gordon et al., 1992; Stramma and  
211 Peterson, 1990) from the west. Water mass formed during this process spreads to the northwest and intrudes  
212 water from the Benguela Current and enters the subtropical gyre (Peterson and Stramma, 1991). Tracing back to  
213 the origin of ESACW, it can be considered as partly originating from WSACW, but since water from Indian  
214 Ocean is added by the Agulhas Current we can define WSACW as a new independent STW with characteristic  
215 properties.

216 We choose the meeting region of Agulhas Current and South Atlantic Current ( $30\text{-}40^{\circ}\text{S}$ ,  $0\text{-}20^{\circ}\text{E}$ ) as the  
217 formation area of ESACW and display properties of this SWT. To investigate the properties of ESACW, we also  
218 follow Stramma and England (1999), and choose 200-700m as the core of this water mass. For the properties,  
219 potential density ( $\sigma_{\theta}$ ) between  $26.00$  and  $27.20 \text{ kg m}^{-3}$  and oxygen concentration between 200 and  $240 \mu\text{mol kg}^{-1}$   
220 are used to define ESACW.

221 Figure 6a clearly shows the linear T-S relationship for potential density ( $\sigma_{\theta}$ ) between  $26.00$  and  $27.20 \text{ kg m}^{-3}$ ,  
222 which is consists with the general property of Central Waters (Alvarez et al., 2014; Emery and Meincke, 1986;  
223 Harvey, 1982). As shown in Figure 6b, ESACW exhibits a relative large potential temperature and salinity range  
224 and low nutrient concentrations (especially low in silicate) compared to the AAIW below. The properties in  
225 ESACW are similar to that of WSACW, although with higher nutrient concentrations due to input from the  
226 Agulhas current.

### 227 3.2 The Intermediate Layer

228 The intermediate water masses origins from the upper part of the ocean (i.e. the upper 500m of the water  
229 column) but subduct into intermediate depth (1000-1500m) during their formation process. Similarly to the water  
230 masses of the central layer, currents in this layer play a significant role to influence the distribution and transport  
231 of intermediate water masses. The potential density ( $\sigma_{\theta}$ ) of the intermediate water masses usually is between  
232  $27.00$  and  $27.70 \text{ kg m}^{-3}$ .

233 In the Atlantic Ocean we find two main intermediate water masses: SAIW that originates from the north and  
234 AAIW that originates from the south, Figure 8. These two water masses are formed in the surface of sub-polar  
235 region, and then sink during their way towards the lower latitudes.

236 Besides AAIW and SAIW here we also define MOW as an intermediate water mass in the north Atlantic since  
237 the MOW occupies a similar density range as AAIW and SAIW, although the formation is different. Schematic  
238 of main currents in the intermediate layer is shown in Figure 7.



### 239 3.2.1 Antarctic Intermediate Water (AAIW)

240 AAIW is the main water mass in the intermediate depth of the South Atlantic Ocean. This water mass originates  
241 from the surface layer (upper 200m) north of the Antarctic Circumpolar Current (ACC) and east of Drake  
242 Passage (Alvarez et al., 2014; McCartney, 1982). After formation AAIW subducts and spreads northward along  
243 the continental slope of South America (Piola and Gordon, 1989). AAIW can be found through most of the  
244 Atlantic Ocean at the depth between 500 and 1200m, below the layer of central water and above the deep waters  
245 (Talley, 1996). Two characteristic features of AAIW is low salinity and high oxygen concentration (Stramma  
246 and England, 1999).

247 Based on the work by Stramma and England (1999), we choose the region between 55 and 40°S (east of the  
248 Drake Passage) as the formation area of AAIW and look at depths below 200 m so that not only AAIW samples  
249 in the formation area but also some samples during the subduction and spreading in the primary stage are  
250 considered. As for the boundaries between AAIW and surrounding SWTs, including SACW in the north and  
251 NADW in the deep, there are several slightly different definitions. Piola and Georgi (1982) and Talley (1996)  
252 define AAIW to have potential densities between 27.00-27.10 and 27.40 kg/m<sup>3</sup>. Here however we follow  
253 Stramma and England (1999) that define the boundary between AAIW and SACW at  $\sigma_{\theta} = 27.00 \text{ kg m}^{-3}$  and the  
254 boundary between AAIW and NADW at  $\sigma_1 = 32.15 \text{ kg m}^{-3}$ .

255 Although the density difference between AAIW and AABW is significant, in the formation areas, there is a  
256 direct contact between AAIW and AABW near Drake Strait. Since AABW is easily separated from AAIW on  
257 higher silicate concentrations we used silicate concentrations lower than 20  $\mu\text{mol kg}^{-1}$  as a criteria for AAIW.  
258 Furthermore we used these criteria in our selection of AAIW: potential density between 26.95 and 27.50  $\text{kg m}^{-3}$   
259 and pressure within 300m. More criteria are required to identify AAIW with neighboring SWTs, since the  
260 formation area of AAIW is bordered with WSACW in the north and AABW in the south. High oxygen (> 230  
261  $\mu\text{mol kg}^{-1}$ ) is the important sign that distinguishes AAIW from Central Waters (WSACW and ESACW), while  
262 relative high potential temperature (>-0.5 °C) and low silicate (< 30  $\mu\text{mol kg}^{-1}$ ) are differentiated standards  
263 between AAIW and AABW. As shown in Figure 8, most of the AAIW samples have a potential density between  
264  $\sigma_{\theta} = 27.00\text{-}27.40 \text{ kg m}^{-3}$ ; the few exceptions still adhere to the boundary  $\sigma_1 < 32.15 \text{ kg m}^{-3}$ . The characteristics of  
265 AAIW show low salinity, high oxygen and low silicate concentrations compared to SACW and NADW, and low  
266 silicate concentration.

### 267 3.2.2 Subarctic Intermediate Water (SAIW)

268 Subarctic Intermediate Water (SAIW) originates from the surface layer of the western boundary of the North  
269 Atlantic Subpolar Gyre, along the Labrador Current (Lazier and Wright, 1993; Pickart et al., 1997). This SWT  
270 subducts and spreads southeast in the region north of the NAC, advects across the MAR and finally interacts  
271 with MOW, that comes from the eastern Atlantic below ENACW (Arhan, 1990; Arhan and King, 1995). The  
272 formation of SAIW is mixture of two surface water types: Water with high temperature and salinity carried by  
273 the NAC and cold and fresh water from the Labrador Current (Garcia-Ibanez et al., 2015; Read, 2000). In  
274 Garcia-Ibanez et al. (2015), there are two definitions of SAIW, SAIW<sub>6</sub>, which is biased to the warmer and saltier  
275 NAC, and SAIW<sub>4</sub>, which is closer to the cooler and fresher Labrador Current. In this study we discuss the  
276 combination of these two end-members when considering the whole Atlantic Ocean scale.



277 For the spatial boundaries we follow Arhan (1990) and choose longitudes between 35 and 55°W, and latitudes  
278 between 50 and 60 °N, i.e. the region along the Labrador Current and north of the NAC as the formation area of  
279 SAIW (Figure 9a). Within this area we follow Read (2000), and choose potential densities higher than 27.65 kg  
280 m<sup>-3</sup> and potential temperature higher than 4.5 °C to define SAIW. Similar to the definition of AAIW, we include  
281 samples in the depth range from the MLD to 500m as the core layer of SAIW; this pressure includes formation  
282 and subduction of SAIW.

283 In the T-S relationship (Figure 9b), the mixing of two main sources, the warmer and saltier NAC and the colder  
284 and fresher Labrador Current, is evident. In Figure 9c we can see that this SWT is characterized by relative low  
285 potential temperature, salinity and silicate concentration but is high in oxygen

### 286 3.2.3 Mediterranean Overflow Water (MOW)

287 The predecessor of the Mediterranean Overflow Water (MOW) is Mediterranean Waters flowing out through the  
288 Strait of Gibraltar whose main component is modified Levantine Intermediate Water. This is a SWT  
289 characterized by high salinity and temperature and intermediate potential density in the Northeast Atlantic Ocean  
290 (Carracedo et al., 2016). After passing the Strait of Gibraltar, the Mediterranean water mixes rapidly with the  
291 overlying ENACW leading to a sharp decrease of salinity and potential density (Baringer and Price, 1997). In  
292 Gulf of Cadiz, the outflow of MOW turns into two branches: One branch continues to the west, descending the  
293 continental slope, mixing with surrounding water masses in the intermediate depth and influence the water mass  
294 composition as far west as the MAR (Price et al., 1993). The other branch spreads northwards along the coast of  
295 Iberian peninsula and along the European coast and its influence can be observed as far north as the Norwegian  
296 Sea (Reid, 1978, 1979).

297 Here we follow Baringer and Price (1997) and consider MOW to be represented by the high salinity (salinity  
298 between 36.35 and 36.65) samples west of the Strait of Gibraltar as a SWT in the Northeast Atlantic (Figure 10)  
299 although the Mediterranean waters in the Strait are characterized by salinity higher than 38.4).

300 Almost the entire Northeast Atlantic, east of the MAR, intermediate layer is influenced by MOW. As the most  
301 characteristic property of MOW is the high salinity, we display a salinity section plot (Figure 10d) of A05 cruise  
302 from 2005 (74AB2005050), where the high salinity of MOW can be seen and how the high salinity core erodes  
303 westward towards the MAR. The high potential temperature and salinity compared to other water samples at  
304 same depth, and the characteristically low and nutrient concentrations are evident in Figure 10b. Due to the  
305 limited number of samples (less than 200) within our definition of MOW in GLODAPv2, we refrain from  
306 showing the histogram. The properties of MOW can be seen in Figure 10 and Table 3.

### 307 3.3 The Deep and Overflow Layer

308 To the deep and overflow water masses belongs those below the Intermediate Layer, approximately from 1500 to  
309 4000m, with potential densities between 27.7 and 27.88 kg m<sup>-3</sup>. Relative high salinity in the deep (compared to  
310 the intermediate and bottom waters) is another significant property. The source region of these waters is confined  
311 to the North Atlantic, the formation areas and main currents in this layer are shown in Figure 11. The southward  
312 flow of NADW in the North Atlantic, as well as northward flow of AABW in the South Atlantic are



313 indispensable components of Atlantic Meridional Overturning Circulation (AMOC) (Lynch-Stieglitz et al.,  
314 2007) (Broecker and Denton, 1989; Elliot et al., 2002).

315 The North Atlantic Deep Water (NADW) is the main water mass in this layer. NADW is mainly formed in the  
316 Labrador Sea and Irminger Basin in relative high latitude region in North Atlantic by mixing of Labrador Sea  
317 Water and the two variations of overflow waters; ISOW and DSOW. We make a distinction of upper and lower  
318 NADW, the upper portion origins from LSW and lower portion origins from ISOW and DSOW. From the  
319 formation area, NADW spreads to the south mainly with the Deep Western Boundary Current (DWBC) (Dengler  
320 et al., 2004), through the most Atlantic Ocean until  $\sim 50^\circ\text{S}$  where it meets Antarctic Circumpolar Current.  
321 During the south way along DWBC, NADW also spreads significantly in the zonal direction, so that we can find  
322 NADW in the whole Atlantic basin at these densities (Lozier, 2012).

323 Both Denmark Strait Overflow Water (DSOW) and Iceland-Scotland Overflow water (ISOW) originate from  
324 Arctic Ocean and the Nordic Seas. In North Atlantic, these two water masses sink and flow west and east of  
325 Iceland respectively, and finally, they meet and mix with each other in the Irminger Basin (Stramma et al., 2004;  
326 Tanhua et al., 2005). As two main contributions to the formation of lower portion of NADW, they play a  
327 significant role in AMOC. Here we show our analysis based on GLODAPv2 database and discuss DSOW and  
328 ISOW separately.

### 329 **3.3.1 Labrador Sea Water (LSW)**

330 As an important water mass by its own virtue and for the formation of North Atlantic Deep Water (NADW),  
331 LSW is predominant in mid-depth (between 1000m and 2500m depth) in the Labrador Sea region (Elliot et al.,  
332 2002). LSW is characterized by relative low salinity (lower than 34.9) and high oxygen concentration ( $\sim 290$   
333  $\mu\text{mol kg}^{-1}$ ) (Talley and McCartney, 1982). Another important criterion of LSW is the potential density ( $\sigma_\theta$ ), that  
334 ranges from 27.68 to 27.88  $\text{kg m}^{-3}$  (Clarke and Gascard, 1983; Gascard and Clarke, 1983; Kieke et al., 2006;  
335 Stramma et al., 2004). In the large spatial scale, LSW can be considered as one water mass (Dickson and Brown,  
336 1994), however significant differences of different “vintages” of LSW exist (Kieke et al., 2006; Stramma et al.,  
337 2004). LSW can broadly be divided into upper Labrador Sea Water (uLSW) and classic Labrador Sea Water  
338 (cLSW) with the boundary between them at potential density of 27.74  $\text{kg m}^{-3}$  (Kieke et al., 2007; Kieke et al.,  
339 2006; Smethie and Fine, 2001).

340 The following results show our analysis based on GLODAPv2 in the Labrador Sea and Irminger Basin, west of  
341 Mid-Atlantic-Ridge. For the purpose of our analysis (the whole scale of the Atlantic Ocean) we consider LSW as  
342 one integral water mass. Although the Labrador Sea is located in North Atlantic between the Labrador Peninsula  
343 and Greenland, for this analysis we consider the formation region of LSW (Figure 12a). Within this geographical  
344 region we follow the definition from Clarke and Gascard (1983) and Stramma and England (1999), defining  
345 LSW as samples with potential density ( $\sigma_\theta$ ) between 27.68 to 27.88  $\text{kg m}^{-3}$  (Figure 12b) in the depth range of  
346 500-2000m (Elliot et al., 2002).

347 Obvious characteristics of LSW are relative low salinity and high oxygen concentration is obvious. Figure 12c  
348 shows the histogram of all samples that we consider to represent LSW in this analysis. The relatively large  
349 spread in properties is indicative of the different “vintages” of LSW, in particular the bi-modal distribution of  
350 density, and partly for oxygen.





### 351 **3.3.2 Denmark Strait Overflow Water (DSOW)**

352 In North Atlantic, a number of water masses from the Arctic Ocean and the Nordic Seas flows through Denmark  
353 Strait west of Iceland. At the sill of the Denmark Strait and during the descent into the Irminger Sea these water  
354 masses undergo intense mixing. Here we use samples from the Irminger Sea with potential density higher than  
355  $27.88 \text{ kg m}^{-3}$  (Tanhua et al., 2005) for our definition of DSOW. In addition we require the silicate concentration  
356 to be lower than  $11 \text{ } \mu\text{mol kg}^{-1}$  to distinguish DSOW from NEABW, which has a high silicate concentration.

357 As shown in Figure 13b DSOW is mostly found close to the bottom between 2000 and 4000m, as expected for  
358 an overflow water. In addition to the high density and low temperature DSOW also has high oxygen  
359 concentration ( $\sim 290\text{-}310 \text{ } \mu\text{mol kg}^{-1}$ ).

### 360 **3.3.3 Iceland-Scotland Overflow Water (ISOW)**

361 The Iceland Scotland Overflow Water, ISOW, flows from the Iceland Sea to the North Atlantic in the region east  
362 of Iceland, mainly through the Faroe-Bank Channel close to the bottom. ISOW flows and turn into two main  
363 branches when passing the Charlie-Gibbs Fracture Zone (CGFZ). The first one flows through the Mid-Atlantic-  
364 Ridge, into the Irminger basin, meets and mixes with DSOW there, and finally joins the lower portion of  
365 NADW. The other branch goes southward and mixes with Northeast Atlantic Bottom Water (NEABW) (Garcia-  
366 Ibanez et al., 2015). The pathway of ISOW closely follows the Mid-Atlantic-Ridge in the Iceland Basin where  
367 also NEABW could be found, characterized by high nutrient and low oxygen concentration. In order to safely  
368 distinguish ISOW from LSW in the region west of MAR, we define ISOW as samples with salinity higher than  
369  $34.95$ , potential density higher than  $27.83 \text{ kg m}^{-3}$ . Figure 14 displays our characterization of ISOW based on  
370 GLODAPv2 in the Iceland Basin, which is consistent from the result in the literature (Garcia-Ibanez et al.,  
371 2015).

### 372 **3.3.4 Upper North Atlantic Deep Water (uNADW)**

373 The uNADW is formed by mixing of mainly ISOW and LSW and we consider this to be a distinct water mass  
374 just south of the Labrador Sea as this region is identified as the formation area of upper and lower NADW  
375 (Dickson and Brown, 1994).

376 We select the region between latitude  $40$  and  $50^\circ\text{N}$ , west of the MAR as the formation area of NADW (Figure  
377 15b) and use the criteria of potential density between  $27.72$  and  $27.82 \text{ kg m}^{-3}$  with depth range from  $1200$  to  
378  $2000\text{m}$  to define the upper NADW (Stramma et al., 2004).

379 As a product of mixing from LSW and ISOW, upper NADW inherits main properties from LSW but also  
380 contains some of characteristics from ISOW. Relative low salinity and high salinity is still significant features of  
381 uNADW. However, as shown in Figure 15d, relatively increased salinity and decreased oxygen concentration  
382 can be found due to the impact from ISOW. Furthermore, ISOW also brings slight increase of nutrients including  
383 silicate, phosphate and nitrate.





### 384 3.3.2 Lower North Atlantic Deep Water (LNADW)

385 We select water samples from the same geographic region as upper NADW to define the lower NADW. Below  
386 the uNADW in this region, ISOW and DSOW (with influence of LSW) mix with each other and form the lower  
387 portion of NADW (Stramma et al., 2004). We use water samples found at depths between 2000 and 3000 m with  
388 potential densities between 27.76 and 27.88 kg m<sup>-3</sup> to define lower NADW.

389 From the data shown on Figure 16d, we can see lower NADW has properties more inclined to ISOW compared  
390 with DSOW. For instance, values of salinity and oxygen concentration are between ISOW and DSOW but  
391 obviously closer to ISOW. The nutrients, lower NADW have almost the same values to ISOW, further verified  
392 this inference. High potential temperature shows that the impact from LSW to lower NADW cannot be ignored.

### 393 3.4 The Bottom Layer

394 We define bottom waters as the densest water masses that occupy the lowest layers of the water column,  
395 typically below 4000 m depth and with potential densities higher than 27.88 kg m<sup>-3</sup>. These water masses have an  
396 origin in the Southern Ocean (Figure 17) and are also characterized by their high silicate concentrations (higher  
397 than 100 μmol kg<sup>-1</sup>), in addition to the high densities.

398 Antarctic Bottom Water (AABW) is the main water mass in the bottom layer, and is formed in the Weddell Sea  
399 region, south of Antarctic Circumpolar Current (ACC) through mixing of Circumpolar Deep Water (CDW) and  
400 Weddell Sea Bottom Water (WSBW) (van Heuven et al., 2011). After the formation, AABW spreads to the  
401 north across the equator and further northwards until ~40 °N, where we define this water mass as North East  
402 Atlantic Bottom Water (NEABW).

### 403 3.4.1 Antarctic Bottom Water (AABW)

404 Antarctic Bottom Water (AABW) is the main bottom water in the South Atlantic Ocean and is also an important  
405 bottom water mass in the North Atlantic. As one of the important components in Atlantic Meridional  
406 Overturning Circulation (AMOC), AABW spreads northward below 4000m depth, mainly west of Mid-Atlantic-  
407 Ridge (MAR) and plays a significant role in the Thermohaline Circulation (Andrié et al., 2003; Rhein et al.,  
408 1998). The origin of AABW in Atlantic section can be traced back to the Weddell Sea as a product of mixing of  
409 Weddell Sea Bottom Water (WSBW) and Circumpolar Deep Water (CDW) (Alvarez et al., 2014; Foldvik and  
410 Gammelsrod, 1988).

411 The definition of AABW is all water samples formed south of the Antarctic Circumpolar Current (ACC), i.e.  
412 south of 63°S in the Weddell Sea, with neutral density ( $\gamma$ ) larger than 28.27 kg m<sup>-3</sup> (Orsi et al., 1999; Weiss et  
413 al., 1979). As an additional constraint we define AABW as water samples with silicate higher than 120 μmol kg<sup>-1</sup>  
414 to distinguish AABW from other water masses in this region as high silicate is a trade mark characteristic of  
415 AABW. The main source region of AABW is the Weddell Sea.

416 In Figure 18, we can see clearly that there are two main original water masses (red points) in the selected  
417 formation area of AABW (blue points). This result is also consistent with Orsi et al. (1999) and van Heuven et  
418 al. (2011). The first water mass is the relative warm ( $\theta > 0$  °C) remnants from CDW, which comes with the ACC  
419 from the north. The other one, which is the extremely cold Shelf Water ( $\theta < -1.0$  °C) comes as Weddell Sea  
420 Bottom Water (WSBW) from the south. As shown in Figure 18 we find AABW from 1000m to 5500m depth.



421 The characteristic properties of AABW is the low temperature ( $\theta < 0$  °C), salinity ( $< 34.68$ ) and high nutrient  
422 concentration, especially the high silicate concentrations. In Figure 17c we can see a relative complex  
423 distribution of potential temperature, probably due to the mixing between different water masses with quite  
424 different temperatures (warm CDW and cold shelf water) that forms AABW.

#### 425 **3.4.2 Northeast Atlantic Bottom Water (NEABW)**

426 Northeast Atlantic Bottom Water (NEABW), also called lower Northeast Atlantic Deep Water (INEADW in  
427 Garcia-Ibanez et al. (2015)), is mainly found below 4000m depth in the eastern basin of the North Atlantic. This  
428 water mass is an extension of AABW during the way to the north, since the characteristics of AABW changes  
429 significantly on the slow transport north we choose to define this as a new water mass north of the Equator,  
430 similar to the formation of NADW south of the Labrador Sea.

431 To define we choose the region east of the MAR and between the equator and 30 °N, i.e. before NEABW enters  
432 the Iberian Basin, as the formation area (Figure 19). We also use the criteria of water samples from a depth  
433 deeper than 4000m and potential temperature above 1.8 °C. In the T-S diagram of NEABW (Figure 19) we can  
434 see the linear T-S relationship similar to AABW in the Weddell Sea, but with significantly higher potential  
435 temperatures and salinities, roughly 1.95 °C and 34.887, respectively. Most NEABW samples have a potential  
436 density higher than 27.88 kg m<sup>-3</sup> and NEABW is characterized by low potential temperature ( $\theta$ ), low salinity but  
437 high silicate concentration. This shows that NEABW originates from AABW, although most properties have  
438 been changed significantly from the South Atlantic.

#### 439 **3.4.3 Circumpolar Deep Water (CDW) / Warm Deep Water (WDW)**

440 Circumpolar Deep Water (CDW) or, as it is also called, Warm Deep Water (WDW), is the lighter of the two  
441 SWTs that constitutes AABW. In our study we consider water mass that mixes with WSBW directly as CDW  
442 (WDW in van Heuven et al. (2011)) and the region between 55 and 65 °S as the formation area. The origin of  
443 CDW can be tracked to the southward flow of NADW. At about 50°S NADW is deflected upward by AABW  
444 before reaching the ACC area, this NADW mixes with other water masses in ACC and forms a new water mass  
445 called CDW. Then CDW flows further southward and passes the ACC.

446 To specify CDW we selected water samples with from depth between 200 and 1000m in the region east of 60°W  
447 between 55 and 65°S as the core of CDW. We also placed the additional constraints of having salinity lower than  
448 34.64 and potential density higher than 27.80 kg m<sup>-3</sup>. The properties of CDW are shown in Figure 20. Similar to  
449 other bottom SWTs, CDW is characterized by high nutrient concentrations (silicate, phosphate and nitrate) and  
450 low oxygen concentration. The potential temperature of CDW is between 0 and 1 °C while the potential density  
451 is larger than 27.8 kg m<sup>-3</sup>, and the salinity higher than 34.63.

#### 452 **3.4.4 Weddell Sea Bottom Water (WSBW)**

453 The Weddell Sea Bottom Water (WSBW) is the denser SWT that takes part in the formation of AABW. Similar  
454 to CDW, WSBW is also formed in the Weddell Sea region, relative warm water ( $\sigma_{\theta} > 0$  °C) flows southward  
455 and cools down to  $\sigma_{\theta}$  lower than -1°C by mixing with extremely cold shelf water that is transported down along



456 the continental slop. WSBW is thus formed in the Weddell Sea basin below the depth of 3000m, before it meets  
457 and mixes with CDW/WDW. Compared with CDW, its low potential temperature is a significant property of  
458 WSBW (van Heuven et al., 2011).

459 We follow van Heuven et al. (2011) and choose water samples in the latitudinal boundaries of 55 - 65 °S in the  
460 Weddell Sea with pressures larger than 3000 m as the formation core area. We additionally constrain our  
461 selection to samples with potential temperature lower than -0.7 °C and silicate higher than 105 µmol/kg. The  
462 properties of WSBW are shown in Figures 21a and b. In addition to the physical properties, such as low potential  
463 temperature and high potential density, WSBW has high nutrient concentrations, but dislike CDW, WSBW has  
464 high oxygen concentration.

#### 465 **4. Discussion**

466 We have defined Atlantic Ocean Water Masses (WMs) in their formation area as source water types (SWTs) in a  
467 7-dimensional hydrochemical space. The properties of SWTs are important since this is the fundamental basis to  
468 label and investigate water mass transport, distribution and mixing. Table 3 provides an overview of the  
469 properties, and the standard deviation, of the 16 Atlantic Ocean SWTs considered in this study. We used seven  
470 often measured hydrochemical and physical variables to characterize 16 main SWTs in the Atlantic Ocean. To  
471 guide the water mass descriptions we divided the distribution of SWTs into four main vertical layers roughly  
472 separated by potential density in the shallow and concentration of silicate in the deep southern Hemisphere. The  
473 upper layer ( $\sigma_{\theta} < 27.00 \text{ kg m}^{-3}$ ) occupies the most shallow layer (typically down to about 500 m depth) of the  
474 ocean below the mixed layer, that we do not consider in this analysis. The upper layer is occupied by central  
475 waters: ENACW, WNACW, WSACW and ESACW, mainly characterized by relative high potential temperature  
476 and salinity. The intermediate layer is situated between the upper layer and the deep layer at roughly 1000 and  
477 2000m depth. Of the three SWTs in this layer, AAIW and SAIW are both characterized have relative low  
478 salinity and temperature, while the MOW has high salinity and temperature. In the deep and overflow layer  
479 between roughly 2000 and 4000m we find SWTs with an origin in the north Atlantic. The bottom layer is  
480 occupied by SWTs with a southern origin; these are very cold SWTs with high densities and silicate  
481 concentrations.

482 In Figure 22 we show an overview of the position of the SWTs in a Salinity-Temperature plot where we plotted  
483 the SWTs from the different layers in different colors. It is obvious that a range of additional variables other than  
484 temperature and salinity is helpful, if not necessary, to reliable distinguish different water masses from each  
485 other, and to calculate the mixing ratios of water masses in a water sample with a particular characteristic.

486 The here presented characteristics and (property value and the standard deviation) of Atlantic Ocean SWTs is  
487 intended to guide water mass analysis of hydrographic data.

488



489 **Acknowledgements**

490 This work is based on the comprehensive and detailed data from GLODAP data set throughout the past few  
491 decades. In particular, we are grateful to the efforts from all the scientists and crews on cruises, who generated  
492 funding and dedicated time on committing the collection of data. We also would like to thank the working  
493 groups of GLODAP for their support and information of the collation, quality control and publishing of data.  
494 Their contributions and selfless sharing are prerequisites for the completion of this work. Thanks to the China  
495 Scholarship Council (CSC) for providing funding support to Mian Liu's PhD study in GEOMAR Helmholtz  
496 Centre for Ocean Research Kiel.

497 **References**

- 498 Alvarez, M., Brea, S., Mercier, H., Alvarez-Salgado, X.A.: Mineralization of biogenic materials in the water  
499 masses of the South Atlantic Ocean. I: Assessment and results of an optimum multiparameter analysis. *Prog*  
500 *Oceanogr* 123, 1-23, 2014.
- 501 Andrić, C., Gouriou, Y., Bourlès, B., Ternon, J.F., Braga, E.S., Morin, P., Oudot, C.: Variability of AABW  
502 properties in the equatorial channel at 35°W. *Geophysical Research Letters* 30, n/a-n/a, 2003.
- 503 Arhan, M.: The North Atlantic current and subarctic intermediate water. *J Mar Res* 48, 109-144, 1990.
- 504 Arhan, M., King, B.: Lateral Mixing of the Mediterranean Water in the Eastern North-Atlantic. *J Mar Res* 53,  
505 865-895, 1995.
- 506 Baringer, M.O., Price, J.F.: Mixing and spreading of the Mediterranean outflow. *Journal of Physical*  
507 *Oceanography* 27, 1654-1677, 1997.
- 508 Broecker, W.S., Denton, G.H.: The Role of Ocean-Atmosphere Reorganizations in Glacial Cycles. *Geochimica*  
509 *Et Cosmochimica Acta* 53, 2465-2501, 1989.
- 510 Carracedo, L., Pardo, P.C., Flecha, S., Pérez, F.F.: On the Mediterranean Water Composition. *Journal of*  
511 *Physical Oceanography* 46, 1339-1358, 2016.
- 512 Castro, C.G., Perez, F.F., Holley, S.E., Rios, A.F.: Chemical characterisation and modelling of water masses in  
513 the Northeast Atlantic. *Prog Oceanogr* 41, 249-279, 1998.
- 514 Cianca, A., Santana, R., Marrero, J., Rueda, M., Llinás, O.: Modal composition of the central water in the North  
515 Atlantic subtropical gyre. *Ocean Science Discussions* 6, 2487-2506, 2009.
- 516 Clarke, R.A., Gascard, J.-C.: The Formation of Labrador Sea Water. Part I: Large-Scale Processes. *Journal of*  
517 *Physical Oceanography* 13, 1764-1778, 1983.
- 518 Defant, A.: *Dynamische Ozeanographie*. Springer, 1929.
- 519 Dengler, M., Schott, F.A., Eden, C., Brandt, P., Fischer, J., Zantopp, R.J.: Break-up of the Atlantic deep western  
520 boundary current into eddies at 8° S. *Nature* 432, 1018, 2004.
- 521 Deruijter, W.: Asymptotic Analysis of the Agulhas and Brazil Current Systems. *Journal of Physical*  
522 *Oceanography* 12, 361-373, 1982.
- 523 Dickson, R.R., Brown, J.: The Production of North-Atlantic Deep-Water - Sources, Rates, and Pathways. *J*  
524 *Geophys Res-Oceans* 99, 12319-12341, 1994.
- 525 Elliot, M., Labeyrie, L., Duplessy, J.C.: Changes in North Atlantic deep-water formation associated with the  
526 Dansgaard-Oeschger temperature oscillations (60-10 ka). *Quaternary Science Reviews* 21, 1153-1165, 2002.
- 527 Emery, W.J., Meincke, J.: Global Water Masses - Summary and Review. *Oceanologica Acta* 9, 383-391, 1986.



- 528 Foldvik, A., Gammelsrod, T.: Notes on Southern-Ocean Hydrography, Sea-Ice and Bottom Water Formation.  
529 Palaeogeography Palaeoclimatology Palaeoecology 67, 3-17, 1988.
- 530 Garcia-Ibanez, M.I., Pardo, P.C., Carracedo, L.I., Mercier, H., Lherminier, P., Rios, A.F., Perez, F.F.: Structure,  
531 transports and transformations of the water masses in the Atlantic Subpolar Gyre. Prog Oceanogr 135, 18-36,  
532 2015.
- 533 Gascard, J.-C., Clarke, R.A.: The Formation of Labrador Sea Water. Part II. Mesoscale and Smaller-Scale  
534 Processes. Journal of Physical Oceanography 13, 1779-1797, 1983.
- 535 Gordon, A.L., Weiss, R.F., Smethie, W.M., Warner, M.J.: Thermocline and Intermediate Water Communication  
536 between the South-Atlantic and Indian Oceans. J Geophys Res-Oceans 97, 7223-7240, 1992.
- 537 Haine, T.W.N., Hall, T.M.: A generalized transport theory: Water-mass composition and age. Journal of Physical  
538 Oceanography 32, 1932-1946, 2002.
- 539 Harvey, J.: Theta-S Relationships and Water Masses in the Eastern North-Atlantic. Deep-Sea Research Part a-  
540 Oceanographic Research Papers 29, 1021-1033, 1982.
- 541 Helland-Hansen, B.r.: Nogen hydrografiske metoder. Scand. Naturforsker Mote. Kristiana. Oslo, 1916.
- 542 Jullion, L., Jacquet, S., Tanhua, T.: Untangling biogeochemical processes from the impact of ocean circulation:  
543 First insight on the Mediterranean dissolved barium dynamics. Global Biogeochemical Cycles 31, 1256-1270,  
544 2017.
- 545 Key, R.M., Tanhua, T., Olsen, A., Hoppema, M., Jutterström, S., Schirnack, C., van Heuven, S., Kozyr, A., Lin,  
546 X., Velo, A., Wallace, D.W.R., Mintrop, L.: The CARINA data synthesis project: introduction and overview.  
547 Earth Syst. Sci. Data 2, 105-121, 2010.
- 548 Kieke, D., Rhein, M., Stramma, L., Smethie, W.M., Bullister, J.L., LeBel, D.A.: Changes in the pool of Labrador  
549 Sea Water in the subpolar North Atlantic. Geophysical Research Letters 34, 2007.
- 550 Kieke, D., Rhein, M., Stramma, L., Smethie, W.M., LeBel, D.A., Zenk, W.: Changes in the CFC inventories and  
551 formation rates of Upper Labrador Sea Water, 1997-2001. Journal of Physical Oceanography 36, 64-86, 2006.
- 552 Klein, B., Hogg, N.: On the variability of 18 Degree Water formation as observed from moored instruments at 55  
553 degrees W. Deep-Sea Research Part I-Oceanographic Research Papers 43, 1777-&, 1996.
- 554 Kuhlbrodt, T., Griesel, A., Montoya, M., Levermann, A., Hofmann, M., Rahmstorf, S.: On the driving processes  
555 of the Atlantic meridional overturning circulation. Reviews of Geophysics 45, 2007.
- 556 Lauvset, S.K., Key, R.M., Olsen, A., van Heuven, S., Velo, A., Lin, X., Schirnack, C., Kozyr, A., Tanhua, T.,  
557 Hoppema, M., Jutterström, S., Steinfeldt, R., Jeansson, E., Ishii, M., Perez, F.F., Suzuki, T., Watelet, S.: A new  
558 global interior ocean mapped climatology: the 1° × 1° GLODAP version 2. Earth Syst. Sci. Data 8, 325-340,  
559 2016.
- 560 Lazier, J.R.N., Wright, D.G.: Annual Velocity Variations in the Labrador Current. Journal of Physical  
561 Oceanography 23, 659-678, 1993.
- 562 Lozier, M.S.: Overturning in the North Atlantic. Ann Rev Mar Sci 4, 291-315, 2012.
- 563 Lutjeharms, J.R., van Ballegooyen, R.C.: Anomalous upstream retroflexion in the agulhas current. Science 240,  
564 1770, 1988.
- 565 Lynch-Stieglitz, J., Adkins, J.F., Curry, W.B., Dokken, T., Hall, I.R., Herguera, J.C., Hirschi, J.J., Ivanova, E.V.,  
566 Kissel, C., Marchal, O., Marchitto, T.M., McCave, I.N., McManus, J.F., Mulitza, S., Ninnemann, U., Peeters, F.,  
567 Yu, E.F., Zahn, R.: Atlantic meridional overturning circulation during the Last Glacial Maximum. Science 316,  
568 66-69, 2007.
- 569 McCartney, M.S.: The subtropical recirculation of Mode Waters. J Mar Res 40, 427-464, 1982.



- 570 McCartney, M.S., Talley, L.D.: The subpolar mode water of the North Atlantic Ocean. *Journal of Physical*  
571 *Oceanography* 12, 1169-1188, 1982.
- 572 Montgomery, R.B.: Water characteristics of Atlantic Ocean and of world ocean. *Deep Sea Research (1953)* 5,  
573 134-148, 1958.
- 574 Orsi, A.H., Johnson, G.C., Bullister, J.L.: Circulation, mixing, and production of Antarctic Bottom Water. *Prog*  
575 *Oceanogr* 43, 55-109, 1999.
- 576 Peterson, R.G., Stramma, L.: Upper-Level Circulation in the South-Atlantic Ocean. *Prog Oceanogr* 26, 1-73,  
577 1991.
- 578 Pickart, R.S., Spall, M.A., Lazier, J.R.N.: Mid-depth ventilation in the western boundary current system of the  
579 sub-polar gyre. *Deep-Sea Research Part I-Oceanographic Research Papers* 44, 1025+,1997.
- 580 Piola, A.R., Georgi, D.T.: Circumpolar properties of Antarctic intermediate water and Subantarctic Mode Water.  
581 *Deep Sea Research Part A. Oceanographic Research Papers* 29, 687-711, 1982.
- 582 Piola, A.R., Gordon, A.L.: Intermediate Waters in the Southwest South-Atlantic. *Deep-Sea Research Part a-*  
583 *Oceanographic Research Papers* 36, 1-16, 1989.
- 584 Pollard, R.T., Griffiths, M.J., Cunningham, S.A., Read, J.F., Perez, F.F., Rios, A.F.: Vivaldi 1991-A study of the  
585 formation, circulation and ventilation of Eastern North Atlantic Central Water. *Prog Oceanogr* 37, 167-192, 1996.
- 586 Pollard, R.T., Pu, S.: Structure and Circulation of the Upper Atlantic Ocean Northeast of the Azores. *Prog*  
587 *Oceanogr* 14, 443-462, 1985.
- 588 Price, J.F., Baringer, M.O., Lueck, R.G., Johnson, G.C., Ambar, I., Parrilla, G., Cantos, A., Kennelly, M.A.,  
589 Sanford, T.B.: Mediterranean outflow mixing and dynamics. *Science* 259, 1277-1282, 1993.
- 590 Prieto, E., Gonzalez-Pola, C., Lavin, A., Holliday, N.P.: Interannual variability of the northwestern Iberia deep  
591 ocean: Response to large-scale North Atlantic forcing. *J Geophys Res-Oceans* 120, 832-847, 2015.
- 592 Read, J.: CONVEX-91: water masses and circulation of the Northeast Atlantic subpolar gyre. *Prog Oceanogr* 48,  
593 461-510, 2000.
- 594 Reid, J.L.: On the middepth circulation and salinity field in the North Atlantic Ocean. *Journal of Geophysical*  
595 *Research: Oceans* 83, 5063-5067, 1978.
- 596 Reid, J.L.: On the contribution of the Mediterranean Sea outflow to the Norwegian-Greenland Sea. *Deep Sea*  
597 *Research Part A. Oceanographic Research Papers* 26, 1199-1223, 1979.
- 598 Rhein, M., Stramma, L., Krahnemann, G.: The spreading of Antarctic bottom water in the tropical Atlantic. *Deep-*  
599 *Sea Research Part I-Oceanographic Research Papers* 45, 507-527, 1998.
- 600 Schaffer, A.J., JACOBSEN, A.W., Mikulicz's syndrome: a report of ten cases. *American Journal of Diseases of*  
601 *Children* 34, 327-346, 1927.
- 602 Smethie, W.M., Fine, R.A.: Rates of North Atlantic Deep Water formation calculated from chlorofluorocarbon  
603 inventories. *Deep-Sea Research Part I-Oceanographic Research Papers* 48, 189-215, 2001.
- 604 Sprintall, J., Tomczak, M.: On the formation of Central Water and thermocline ventilation in the southern  
605 hemisphere. *Deep Sea Research Part I: Oceanographic Research Papers* 40, 827-848, 1993.
- 606 Stramma, L., England, M.H.: On the water masses and mean circulation of the South Atlantic Ocean. *J Geophys*  
607 *Res-Oceans* 104, 20863-20883, 1999.
- 608 Stramma, L., Kieke, D., Rhein, M., Schott, F., Yashayaev, I., Koltermann, K.P.: Deep water changes at the  
609 western boundary of the subpolar North Atlantic during 1996 to 2001. *Deep Sea Research Part I: Oceanographic*  
610 *Research Papers* 51, 1033-1056, 2004.



- 611 Stramma, L., Peterson, R.G.: The South-Atlantic Current. *Journal of Physical Oceanography* 20, 846-859, 1990.
- 612 Talley, L.: Antarctic intermediate water in the South Atlantic, *The South Atlantic*. Springer, pp. 219-238, 1996.
- 613 Talley, L., Raymer, M.: Eighteen degree water variability. *J. Mar. Res* 40, 757-775, 1982.
- 614 Talley, L.D., McCartney, M.S.: Distribution and Circulation of Labrador Sea-Water. *Journal of Physical Oceanography* 12, 1189-1205, 1982.
- 616 Tanhua, T., Olsson, K.A., Jeansson, E.: Formation of Denmark Strait overflow water and its hydro-chemical  
617 composition. *Journal of Marine Systems* 57, 264-288, 2005.
- 618 Tomczak, M.: A multi-parameter extension of temperature/salinity diagram techniques for the analysis of non-  
619 isopycnal mixing. *Prog Oceanogr* 10, 147-171, 1981.
- 620 Tomczak, M.: Some historical, theoretical and applied aspects of quantitative water mass analysis. *J Mar Res* 57,  
621 275-303, 1999.
- 622 Tomczak, M., Godfrey, J.S.: *Regional oceanography: an introduction*. Elsevier, 2013.
- 623 Tomczak, M., Large, D.G.B.: Optimum Multiparameter Analysis of Mixing in the Thermocline of the Eastern  
624 Indian-Ocean. *J Geophys Res-Oceans* 94, 16141-16149, 1989.
- 625 van Heuven, S.M.A.C., Hoppema, M., Huhn, O., Slagter, H.A., de Baar, H.J.W.: Direct observation of  
626 increasing CO<sub>2</sub> in the Weddell Gyre along the Prime Meridian during 1973–2008. *Deep Sea Research Part II:*  
627 *Topical Studies in Oceanography* 58, 2613-2635, 2011.
- 628 Weiss, R.F., Ostlund, H.G., Craig, H.: *Geochemical Studies of the Weddell Sea*. *Deep-Sea Research Part a-*  
629 *Oceanographic Research Papers* 26, 1093-1120, 1979.
- 630 Worthington, L.: The 18 water in the Sargasso Sea. *Deep Sea Research (1953)* 5, 297-305, 1959.
- 631 Wüst, G., Defant, A.: *Atlas zur Schichtung und Zirkulation des Atlantischen Ozeans: Schnitte und Karten von*  
632 *Temperatur, Salzgehalt und Dichte*. W. de Gruyter, 1936.
- 633
- 634



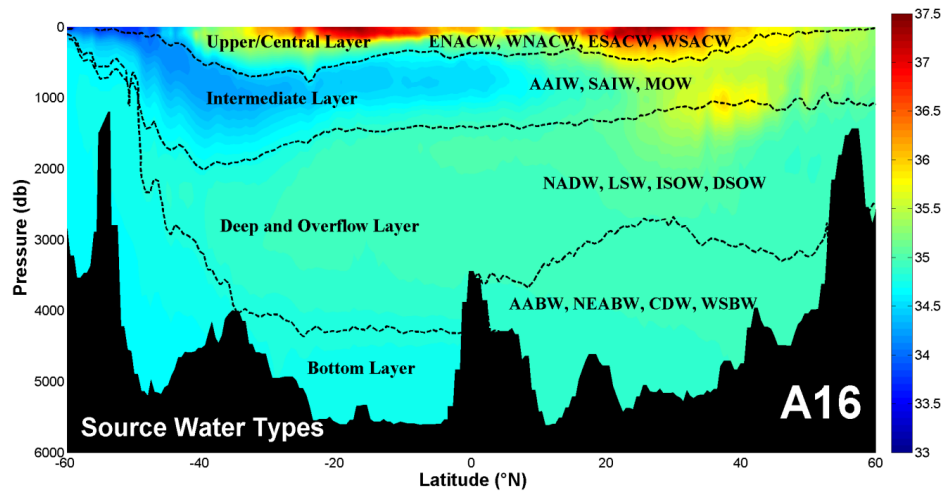


Figure 1: Salinity section from the A16 GO-SHIP cruises in 2013

(Expocode 33RO20130803 in North Atlantic & 33RO20131223 in South Atlantic)

The dashed lines show the four vertical layers divided by potential density except for the boundary between the deep and bottom layers in the south hemisphere which is based on the concentration of silicate.

635

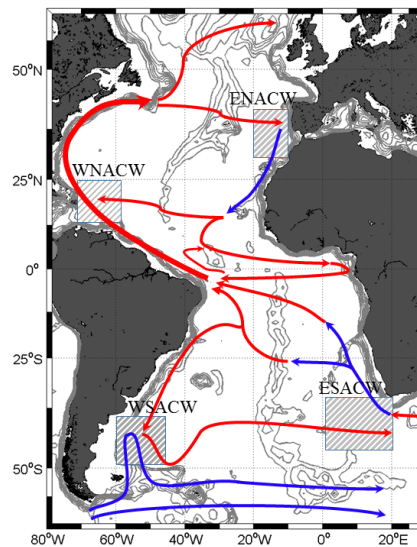


Figure 2: The water mass formation areas and the schematic of main currents (Warm currents in red and cold currents in blue) in the Upper Layer.



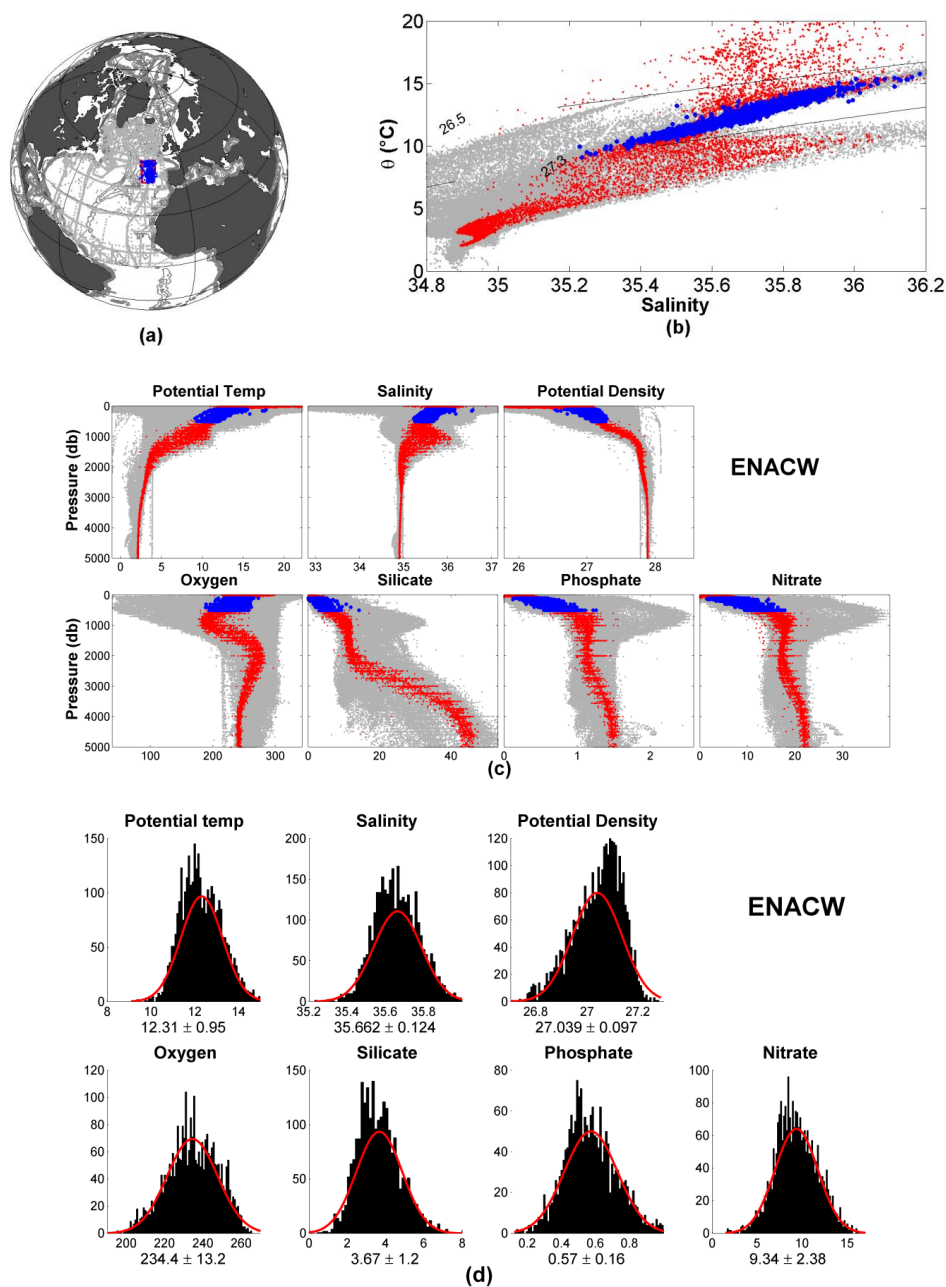


Figure 3: Overview of Eastern North Atlantic Central Water (ENACW):

Panel a) shows the formation area used to define the water mass, panel b) show a T-S diagram and panel c) the distribution of key properties vs. pressure. In panel d) we show bar plots of the data distribution of samples used to define the water mass. Potential Temperature in ( $^{\circ}\text{C}$ ), Potential Density in  $\text{kg}/\text{m}^3$ , Oxygen and nutrients in  $\mu\text{mol}/\text{kg}^3$ . The red Gaussian fit shows mean and  $\sigma$  based on selected data.

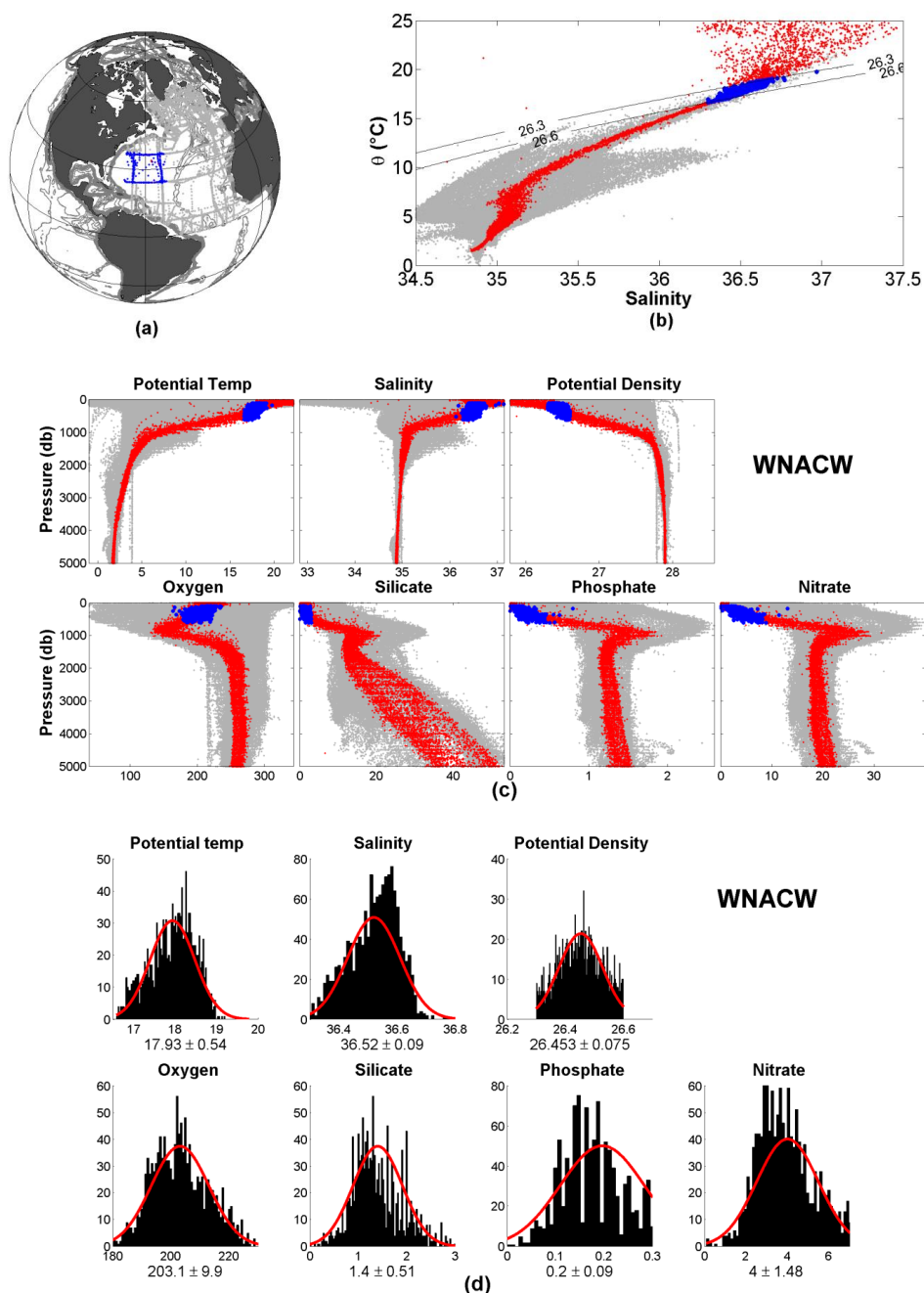


Figure 4: Overview of Western North Atlantic Central Water (WNACW):

Panel a) shows the formation area used to define the water mass, panel b) show a T-S diagram and panel c) the distribution of key properties vs. pressure. In panel d) we show bar plots of the data distribution of samples used to define the water mass. Potential Temperature in ( $^{\circ}\text{C}$ ), Potential Density in  $\text{kg}/\text{m}^3$ , Oxygen and nutrients in  $\mu\text{mol}/\text{kg}^3$ . The red Gaussian fit shows mean and  $\sigma$  based on selected data.

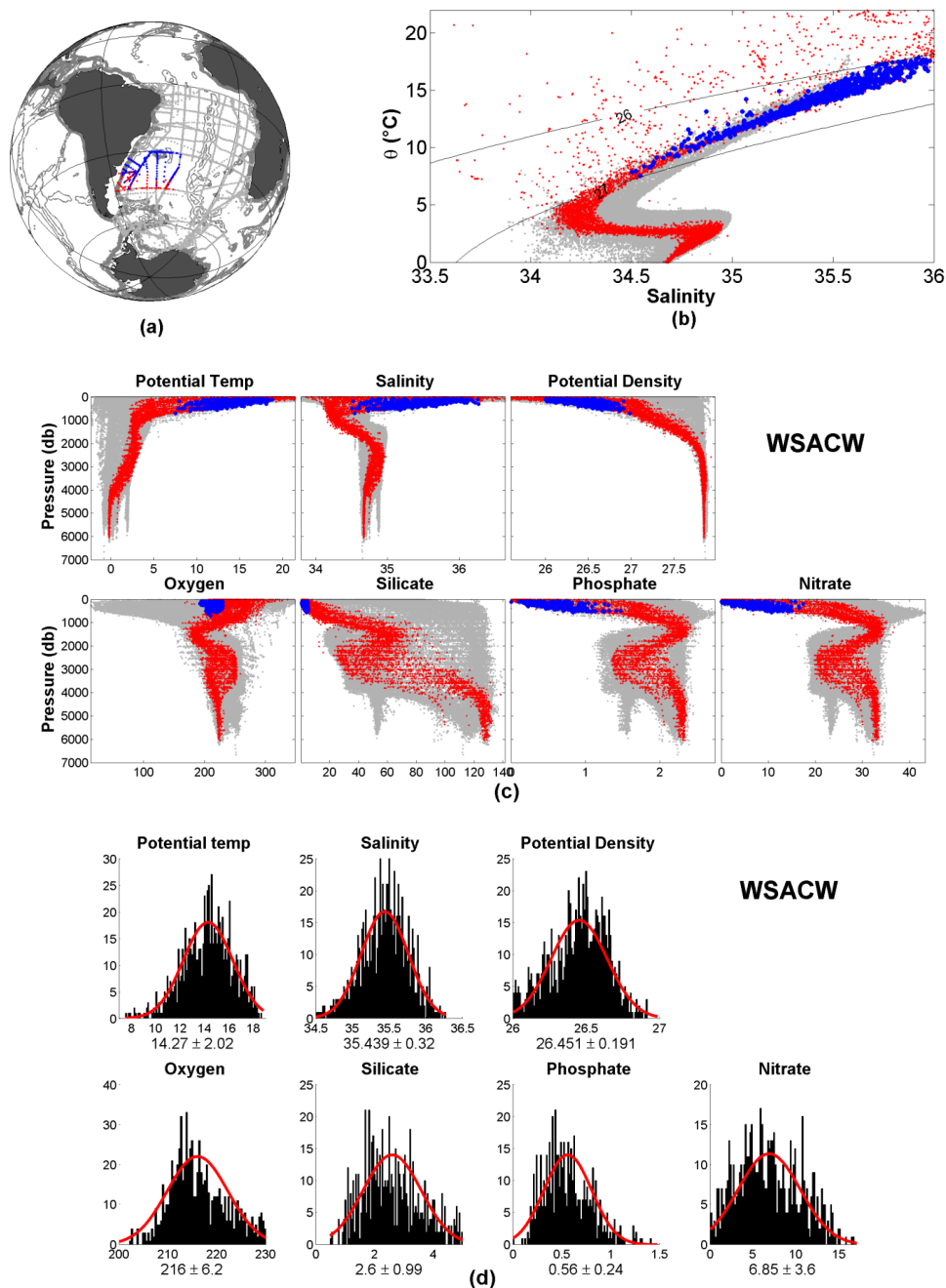
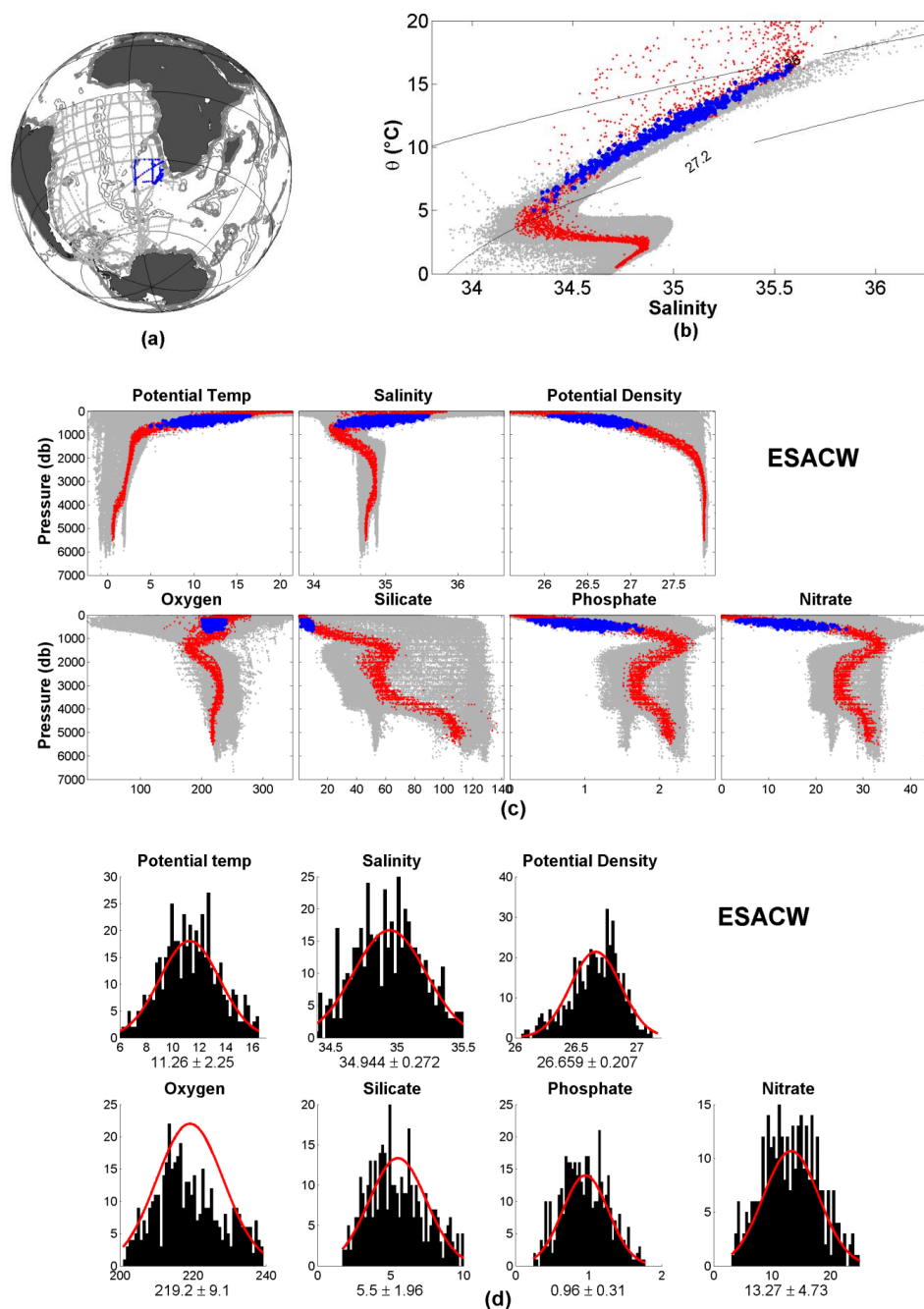


Figure 5: Overview of Western South Atlantic Central Water (WSACW):

Panel a) shows the formation area used to define the water mass, panel b) show a T-S diagram and panel c) the distribution of key properties vs. pressure. In panel d) we show bar plots of the data distribution of samples used to define the water mass. Potential Temperature in (°C), Potential Density in  $\text{kg/m}^3$ , Oxygen and nutrients in  $\mu\text{mol/kg}^3$ . The red Gaussian fit shows mean and  $\sigma$  based on selected data.



**Figure 6: Overview of Eastern South Atlantic Central Water (ESACW):**

Panel a) shows the formation area used to define the water mass, panel b) show a T-S diagram and panel c) the distribution of key properties vs. pressure. In panel d) we show bar plots of the data distribution of samples used to define the water mass. Potential Temperature in ( $^{\circ}\text{C}$ ), Potential Density in  $\text{kg}/\text{m}^3$ , Oxygen and nutrients in  $\mu\text{mol}/\text{kg}^3$ . The red Gaussian fit shows mean and  $\sigma$  based on selected data.

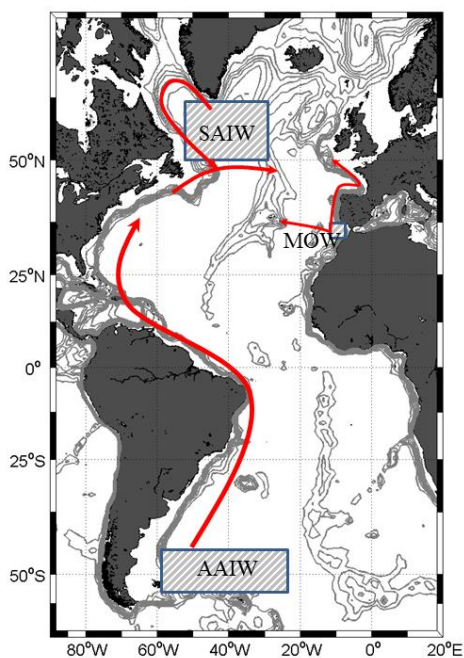


**Figure 7: The water mass formation areas and the schematic of main currents  
in the Intermediate Layer**

637

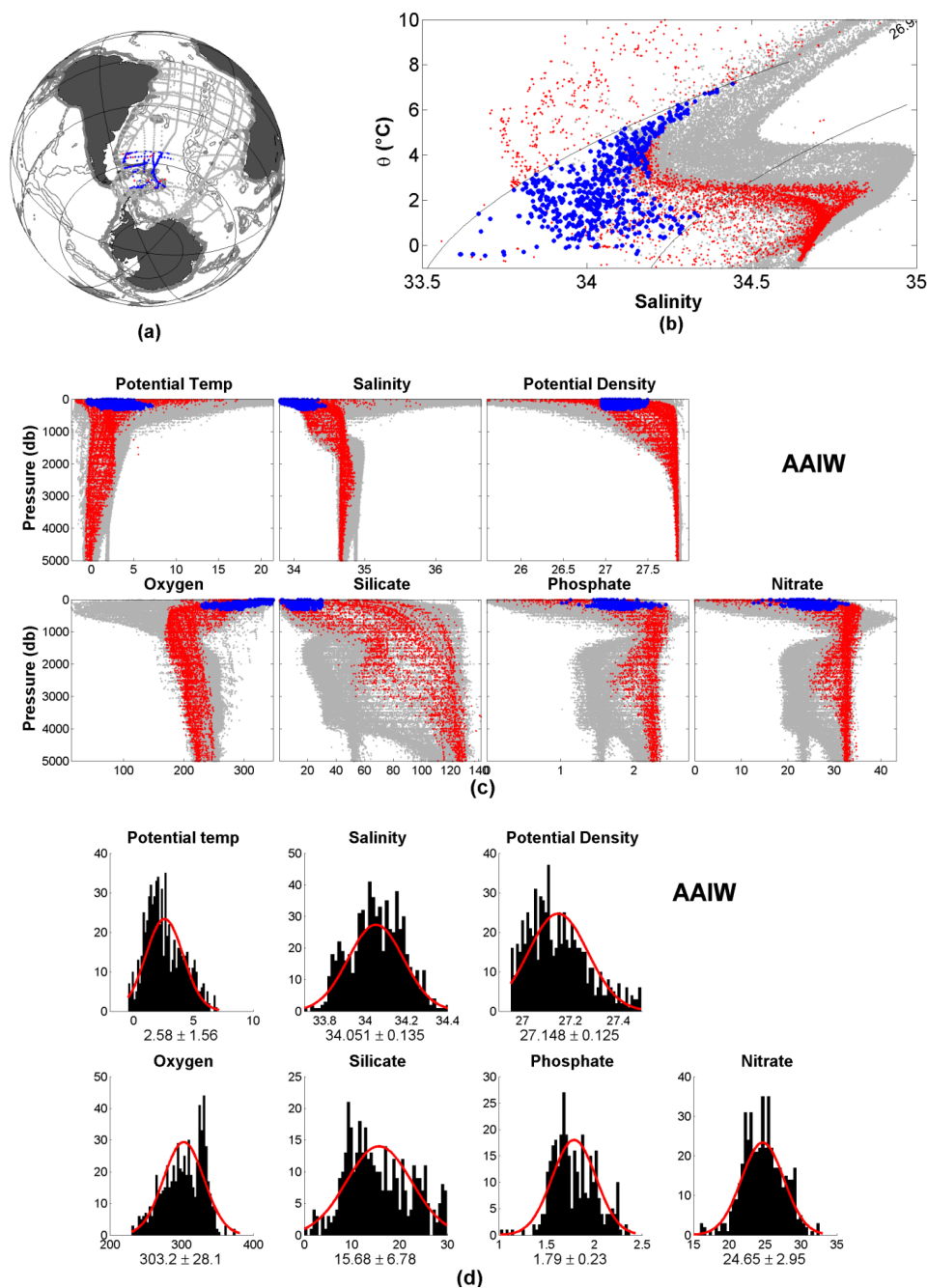


Figure 8: Overview of Antarctic Intermediate Water (AAIW):

Panel a) shows the formation area used to define the water mass, panel b) show a T-S diagram and panel c) the distribution of key properties vs. pressure. In panel d) we show bar plots of the data distribution of samples used to define the water mass. Potential Temperature in (°C), Potential Density in  $\text{kg/m}^3$ , Oxygen and nutrients in  $\mu\text{mol/kg}^3$ . The red Gaussian fit shows mean and  $\sigma$  based on selected data.



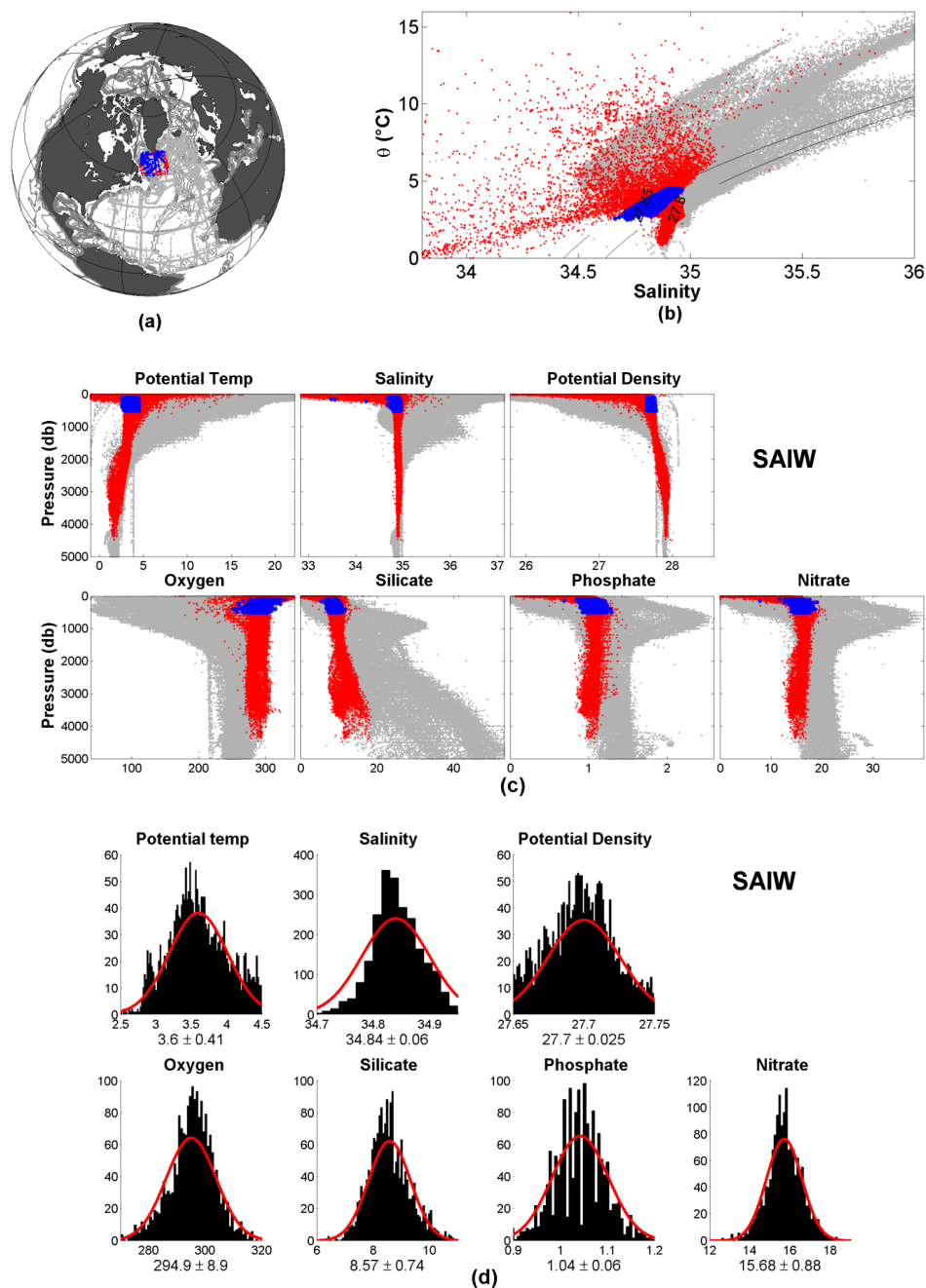


Figure 9: Overview of Subarctic Intermediate Water (SAIW):

Panel a) shows the formation area used to define the water mass, panel b) show a T-S diagram and panel c) the distribution of key properties vs. pressure. In panel d) we show bar plots of the data distribution of samples used to define the water mass. Potential Temperature in (°C), Potential Density in  $\text{kg/m}^3$ , Oxygen and nutrients in  $\mu\text{mol/kg}^3$ . The red Gaussian fit shows mean and  $\sigma$  based on selected data.

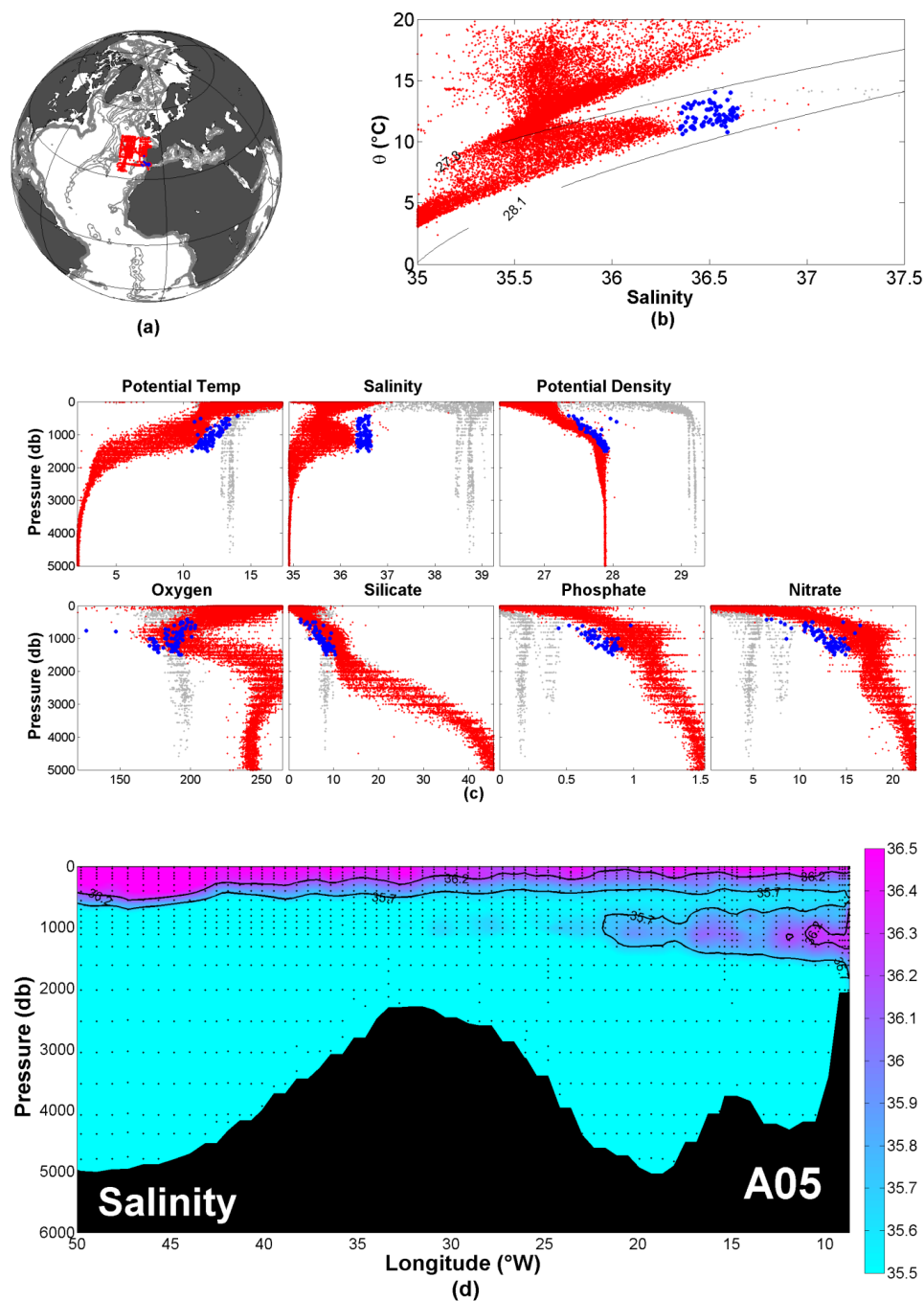
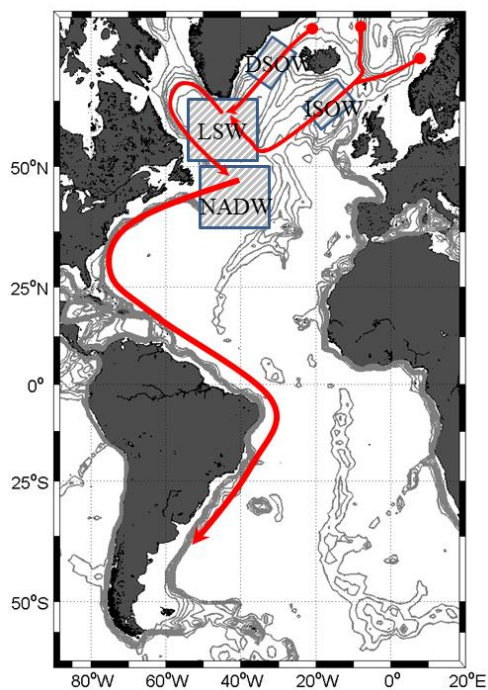


Figure 10: Overview of Mediterranean Overflow Water (MOW):

Panel a) shows the formation area used to define the water mass, panel b) show a T-S diagram and panel c) the distribution of key properties vs. pressure. In panel d) we show the salinity along A05 cruise.





**Figure 11: The water mass formation areas and the schematic of main currents  
in the Deep and Overflow Layer.**

639

640

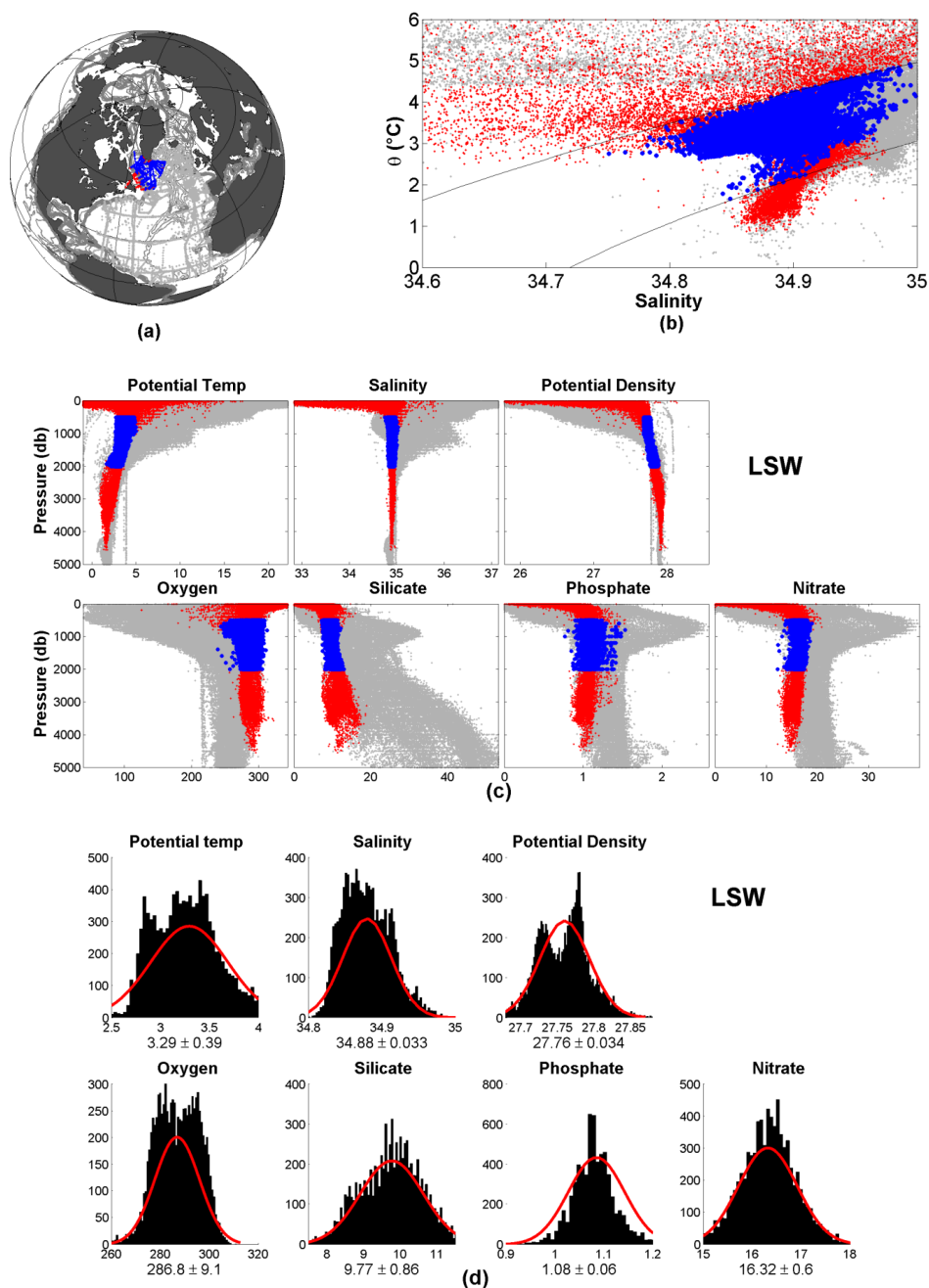


Figure 12: Overview of Labrador Sea Water (LSW):

Panel a) shows the formation area used to define the water mass, panel b) show a T-S diagram and panel c) the distribution of key properties vs. pressure. In panel d) we show bar plots of the data distribution of samples used to define the water mass. Potential Temperature in ( $^{\circ}\text{C}$ ), Potential Density in  $\text{kg}/\text{m}^3$ , Oxygen and nutrients in  $\mu\text{mol}/\text{kg}^3$ . The red Gaussian fit shows mean and  $\sigma$  based on selected data.

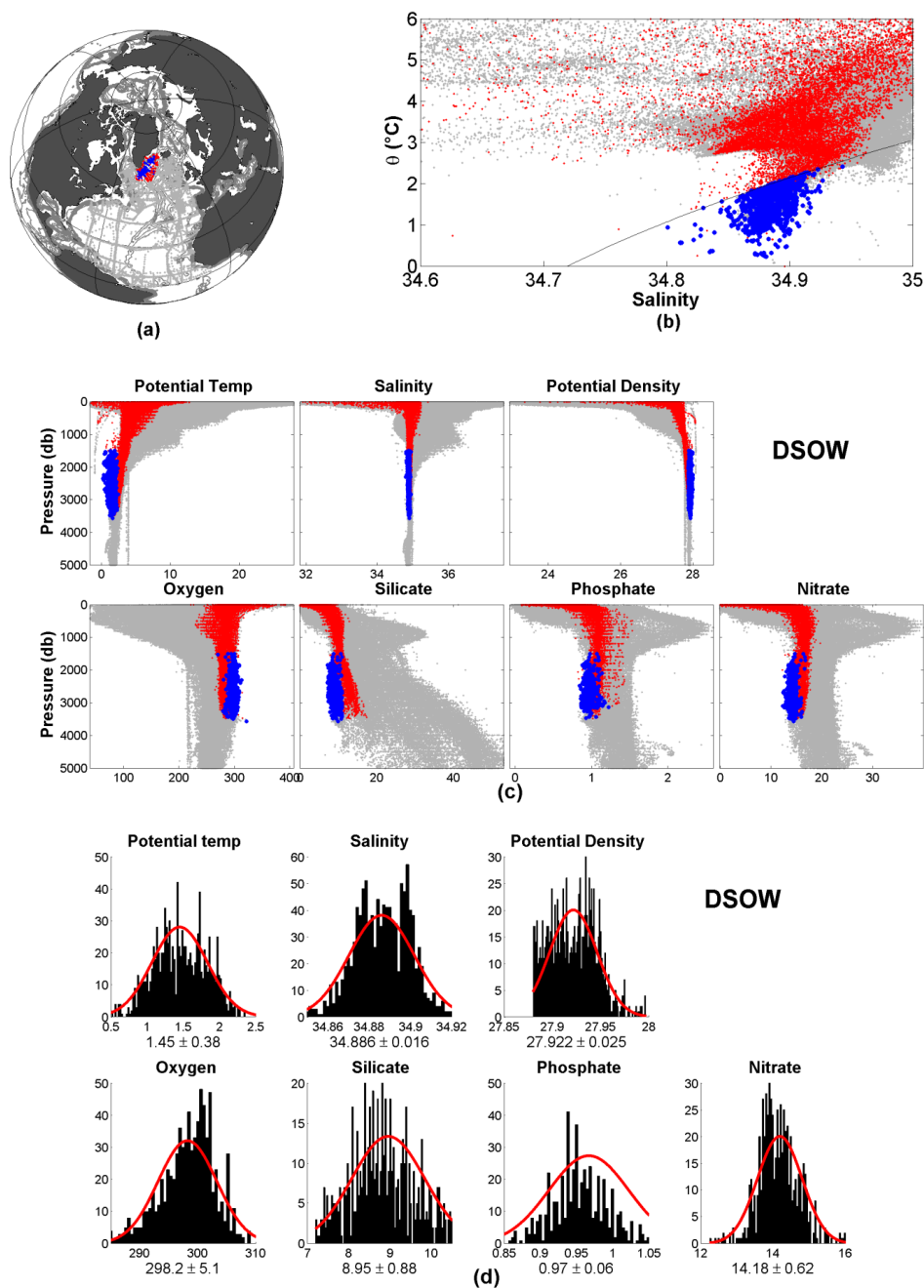


Figure 13: Overview of Denmark Strait Overflow Water (DSOW):

Panel a) shows the formation area used to define the water mass, panel b) show a T-S diagram and panel c) the distribution of key properties vs. pressure. In panel d) we show bar plots of the data distribution of samples used to define the water mass. Potential Temperature in ( $^{\circ}\text{C}$ ), Potential Density in  $\text{kg}/\text{m}^3$ , Oxygen and nutrients in  $\mu\text{mol}/\text{kg}^3$ . The red Gaussian fit shows mean and  $\sigma$  based on selected data.

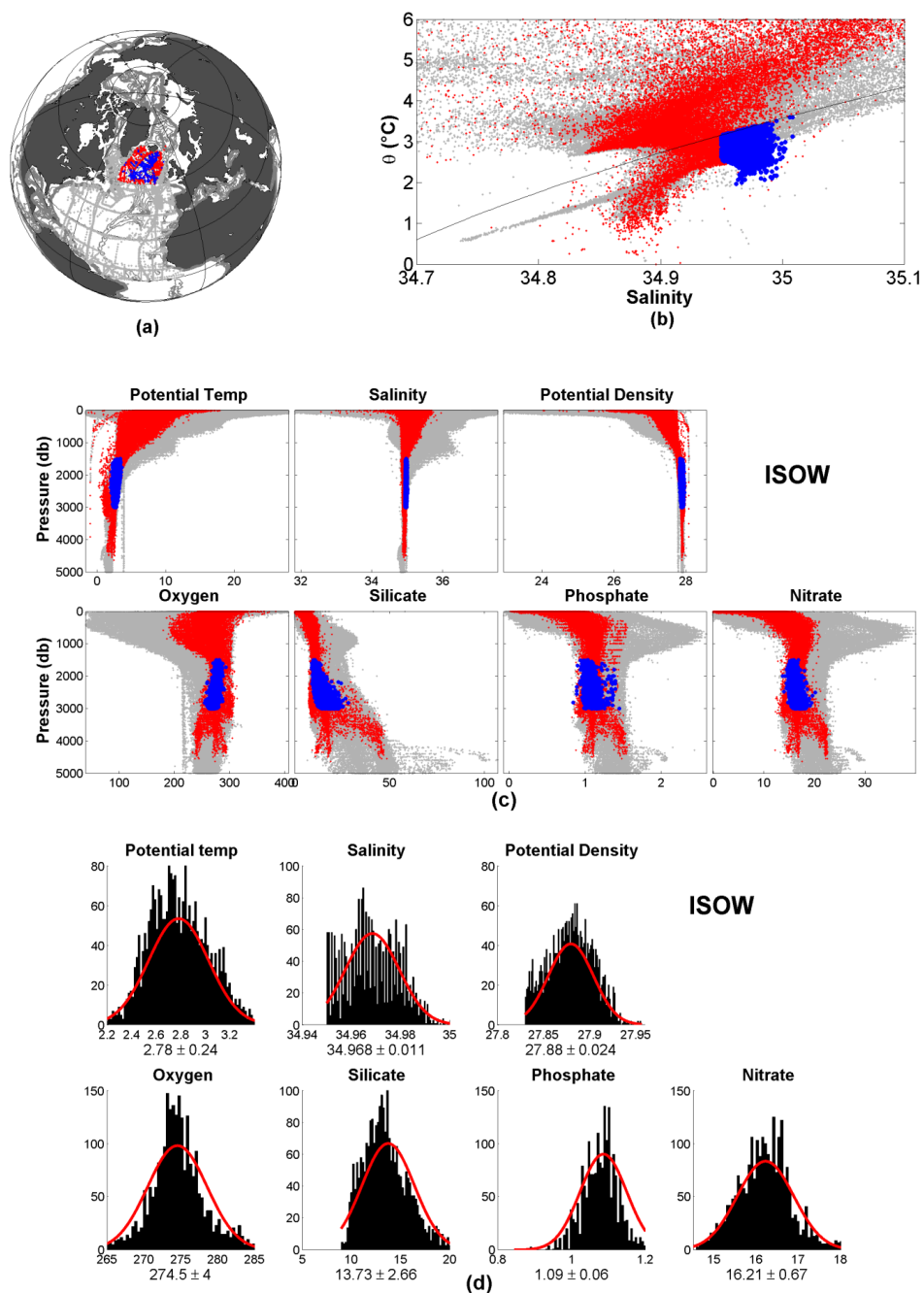
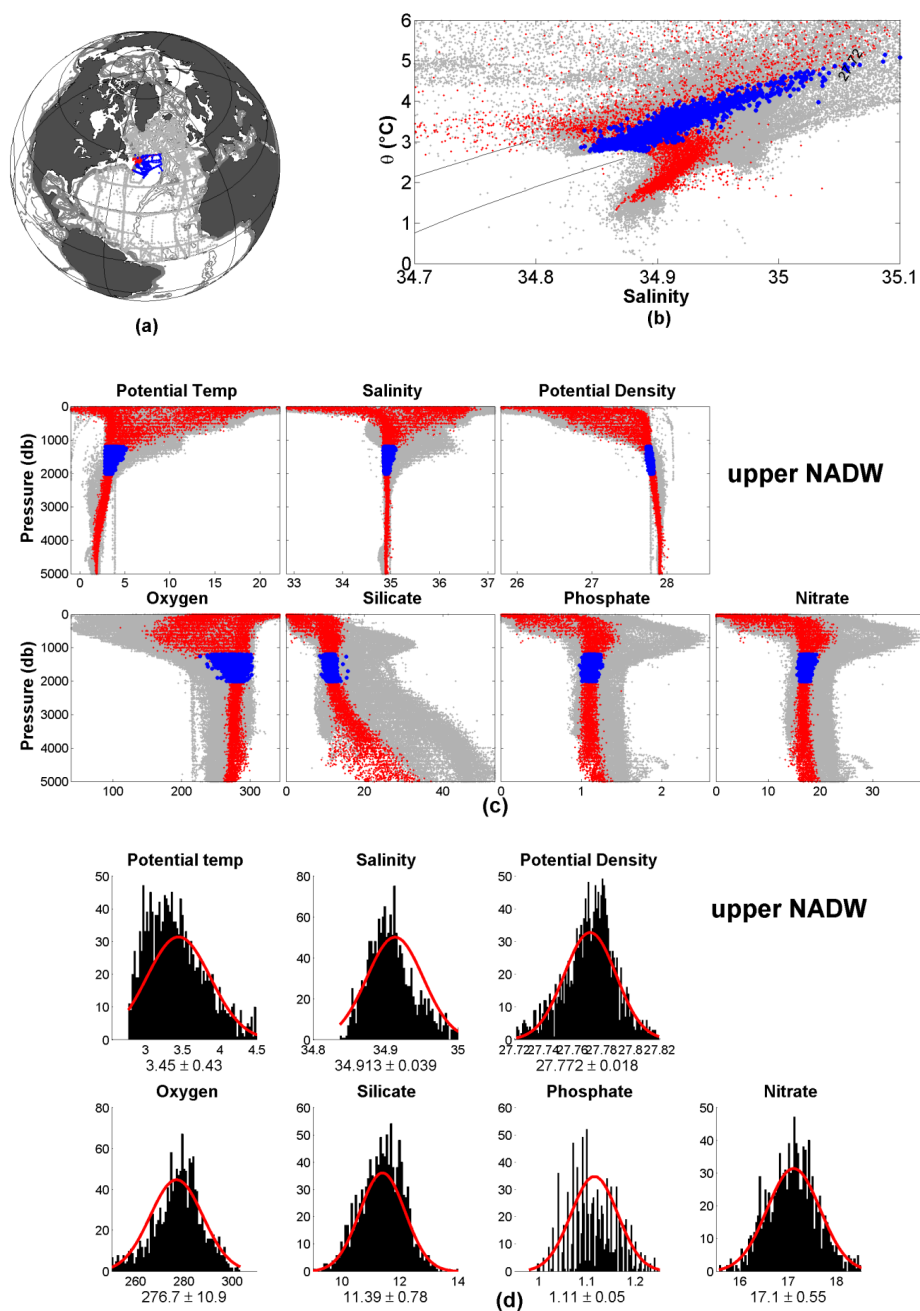


Figure 14: Overview of Iceland-Scotland Overflow Water (ISOW):

Panel a) shows the formation area used to define the water mass, panel b) show a T-S diagram and panel c) the distribution of key properties vs. pressure. In panel d) we show bar plots of the data distribution of samples used to define the water mass. Potential Temperature in (°C), Potential Density in  $\text{kg/m}^3$ , Oxygen and nutrients in  $\mu\text{mol/kg}^3$ . The red Gaussian fit shows mean and  $\sigma$  based on selected data.



**Figure 15: Overview of upper North Atlantic Deep Water (uNADW):**

Panel a) shows the formation area used to define the water mass, panel b) show a T-S diagram and panel c) the distribution of key properties vs. pressure. In panel d) we show bar plots of the data distribution of samples used to define the water mass. Potential Temperature in (°C), Potential Density in  $\text{kg/m}^3$ , Oxygen and nutrients in  $\mu\text{mol/kg}^3$ . The red Gaussian fit shows mean and  $\sigma$  based on selected data.

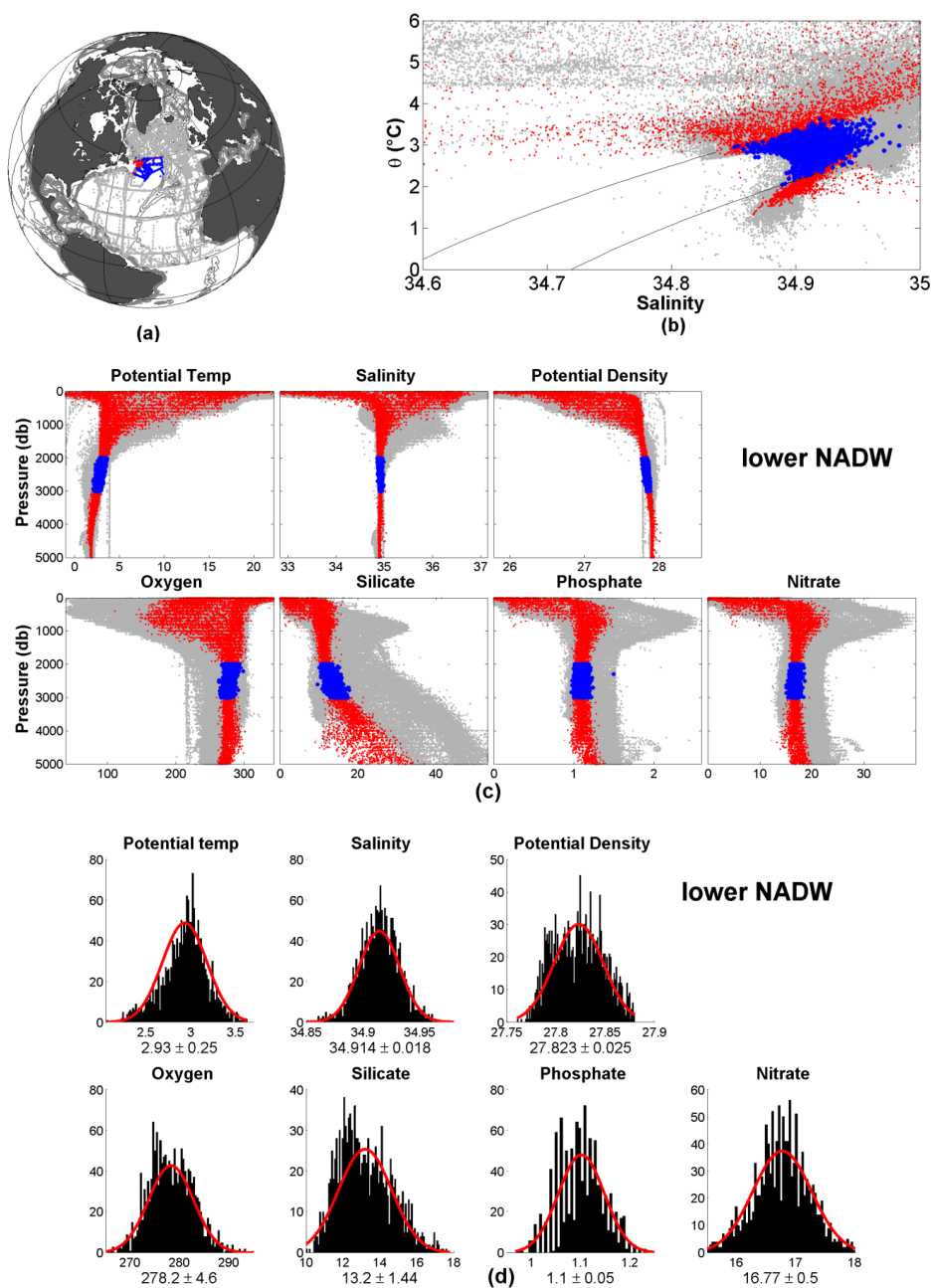


**Figure 16: Overview of lower North Atlantic Deep Water (INADW):**

Panel a) shows the formation area used to define the water mass, panel b) show a T-S diagram and panel c) the distribution of key properties vs. pressure. In panel d) we show bar plots of the data distribution of samples used to define the water mass. Potential Temperature in (°C), Potential Density in kg/m<sup>3</sup>, Oxygen and nutrients in μmol/kg<sup>3</sup>. The red Gaussian fit shows mean and σ based on selected data.



641

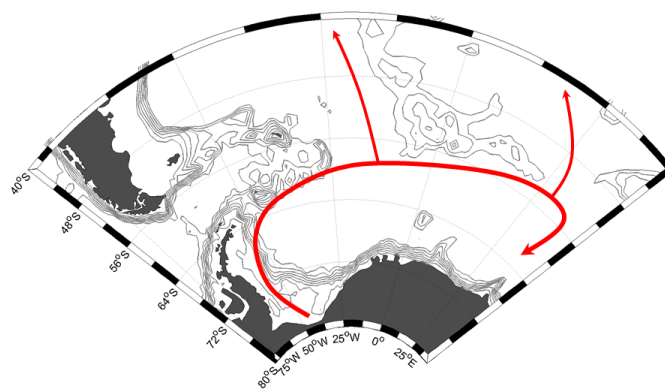


Figure 17: The water mass formation areas and the schematic of main currents in the Bottom Layer

642



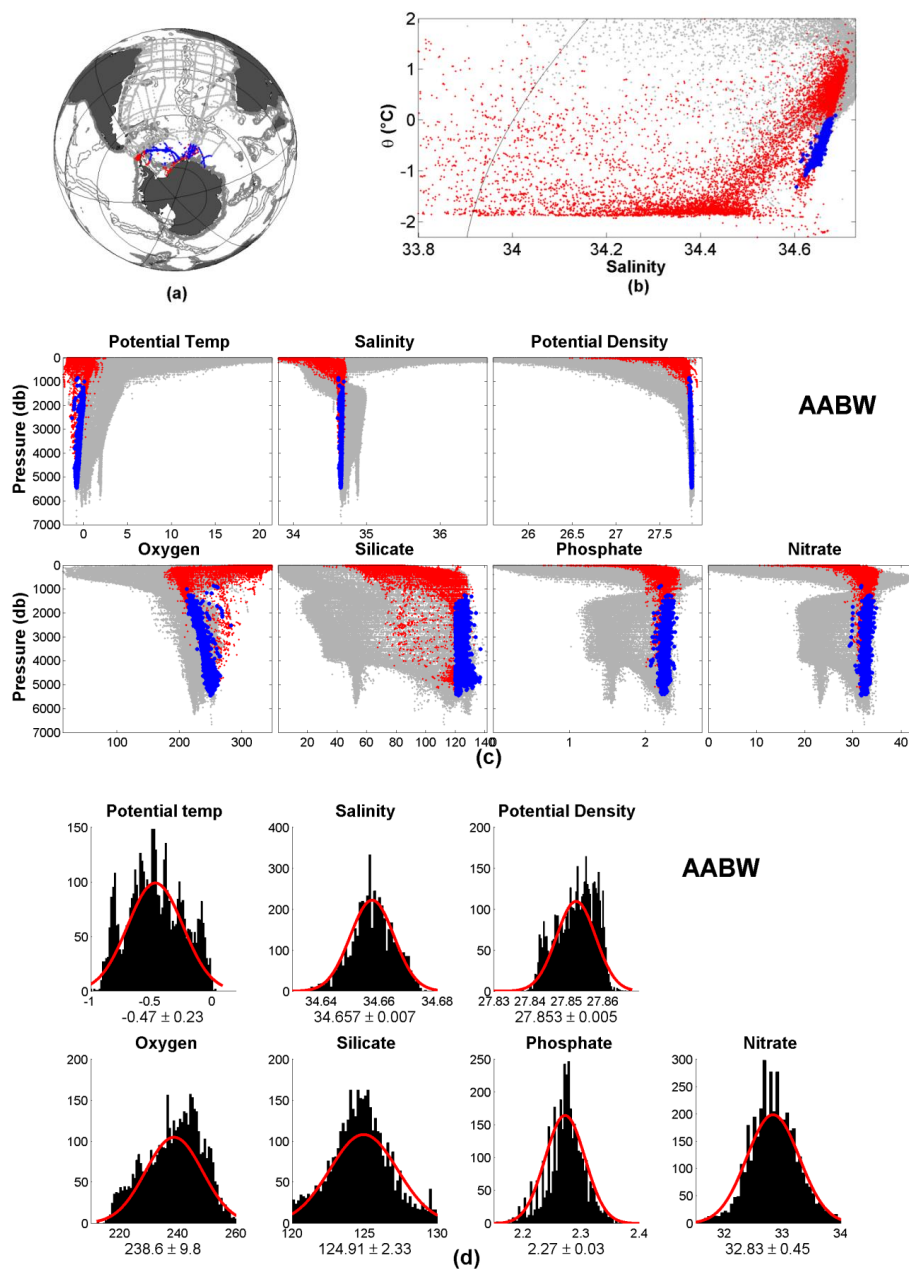


Figure 18: Overview of Antarctic Bottom Water (AABW):

Panel a) shows the formation area used to define the water mass, panel b) show a T-S diagram and panel c) the distribution of key properties vs. pressure. In panel d) we show bar plots of the data distribution of samples used to define the water mass. Potential Temperature in ( $^{\circ}\text{C}$ ), Potential Density in  $\text{kg}/\text{m}^3$ , Oxygen and nutrients in  $\mu\text{mol}/\text{kg}^3$ . The red Gaussian fit shows mean and  $\sigma$  based on selected data.



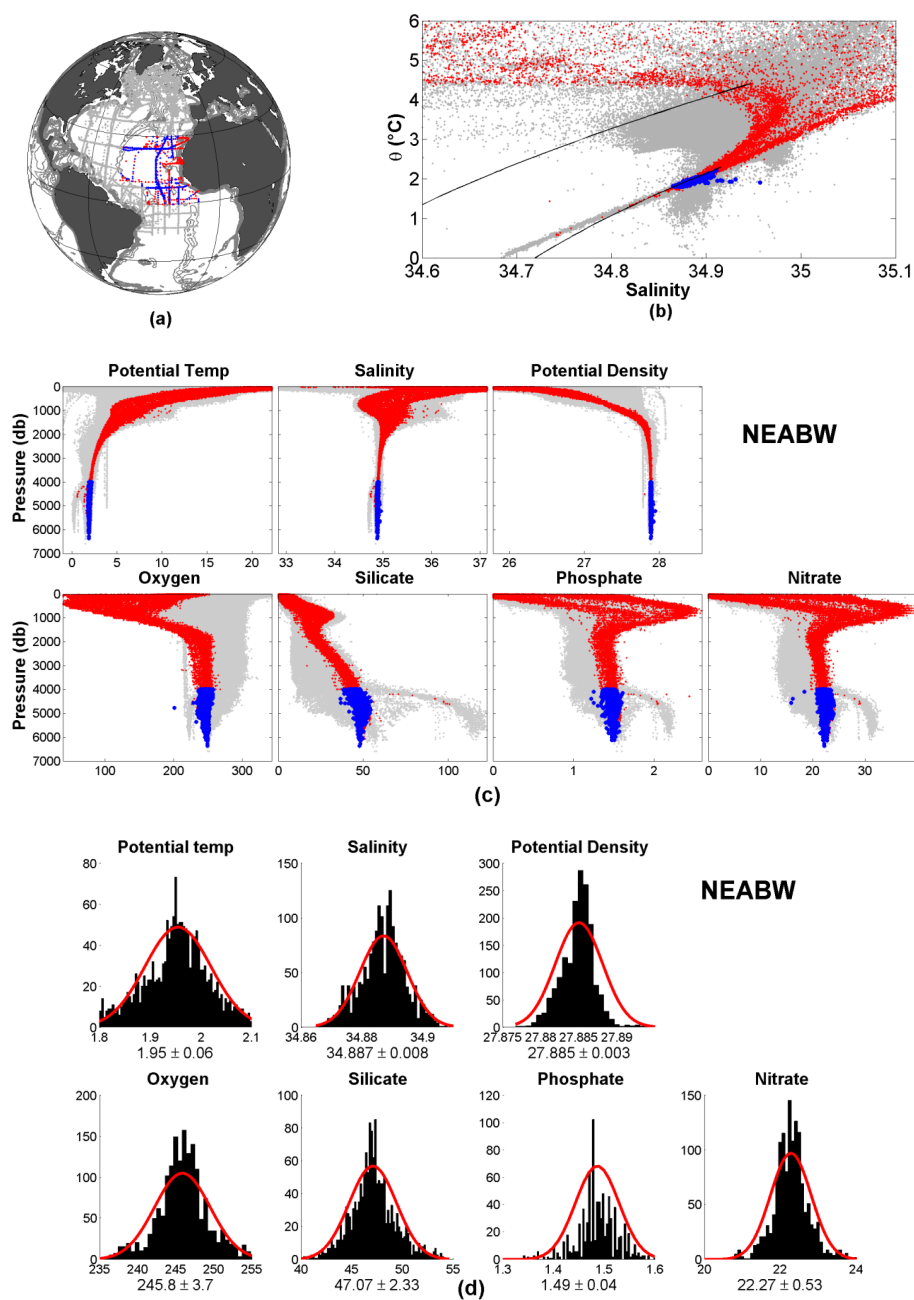
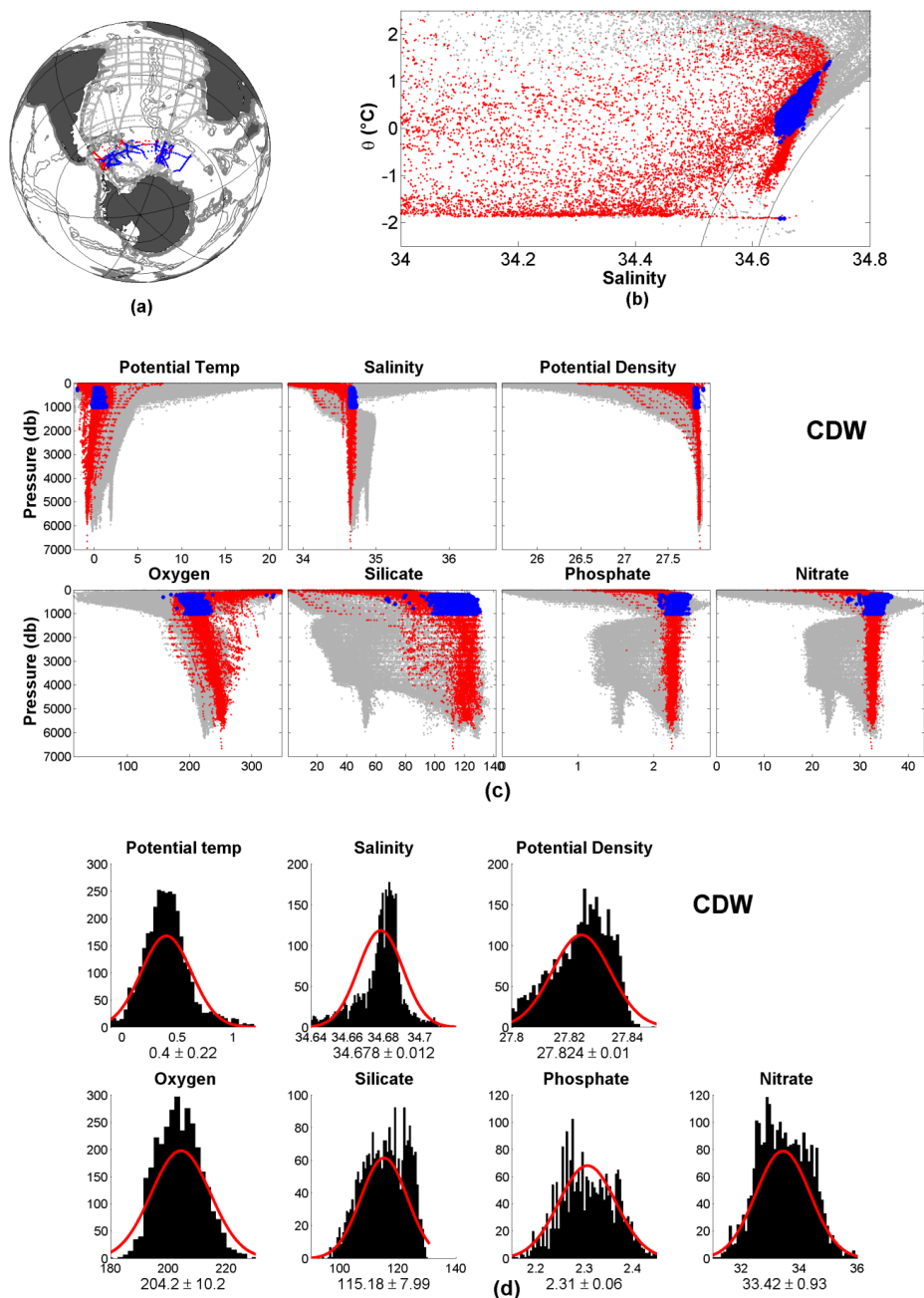


Figure 19: Overview of Northeast Atlantic Bottom Water (NEABW):

Panel a) shows the formation area used to define the water mass, panel b) show a T-S diagram and panel c) the distribution of key properties vs. pressure. In panel d) we show bar plots of the data distribution of samples used to define the water mass. Potential Temperature in ( $^{\circ}\text{C}$ ), Potential Density in  $\text{kg}/\text{m}^3$ , Oxygen and nutrients in  $\mu\text{mol}/\text{kg}^3$ . The red Gaussian fit shows mean and  $\sigma$  based on selected data.



**Figure 20: Overview of Circumpolar Deep Water (CDW):**

Panel a) shows the formation area used to define the water mass, panel b) show a T-S diagram and panel c) the distribution of key properties vs. pressure. In panel d) we show bar plots of the data distribution of samples used to define the water mass. Potential Temperature in ( $^{\circ}\text{C}$ ), Potential Density in  $\text{kg}/\text{m}^3$ , Oxygen and nutrients in  $\mu\text{mol}/\text{kg}^3$ . The red Gaussian fit shows mean and  $\sigma$  based on selected data.

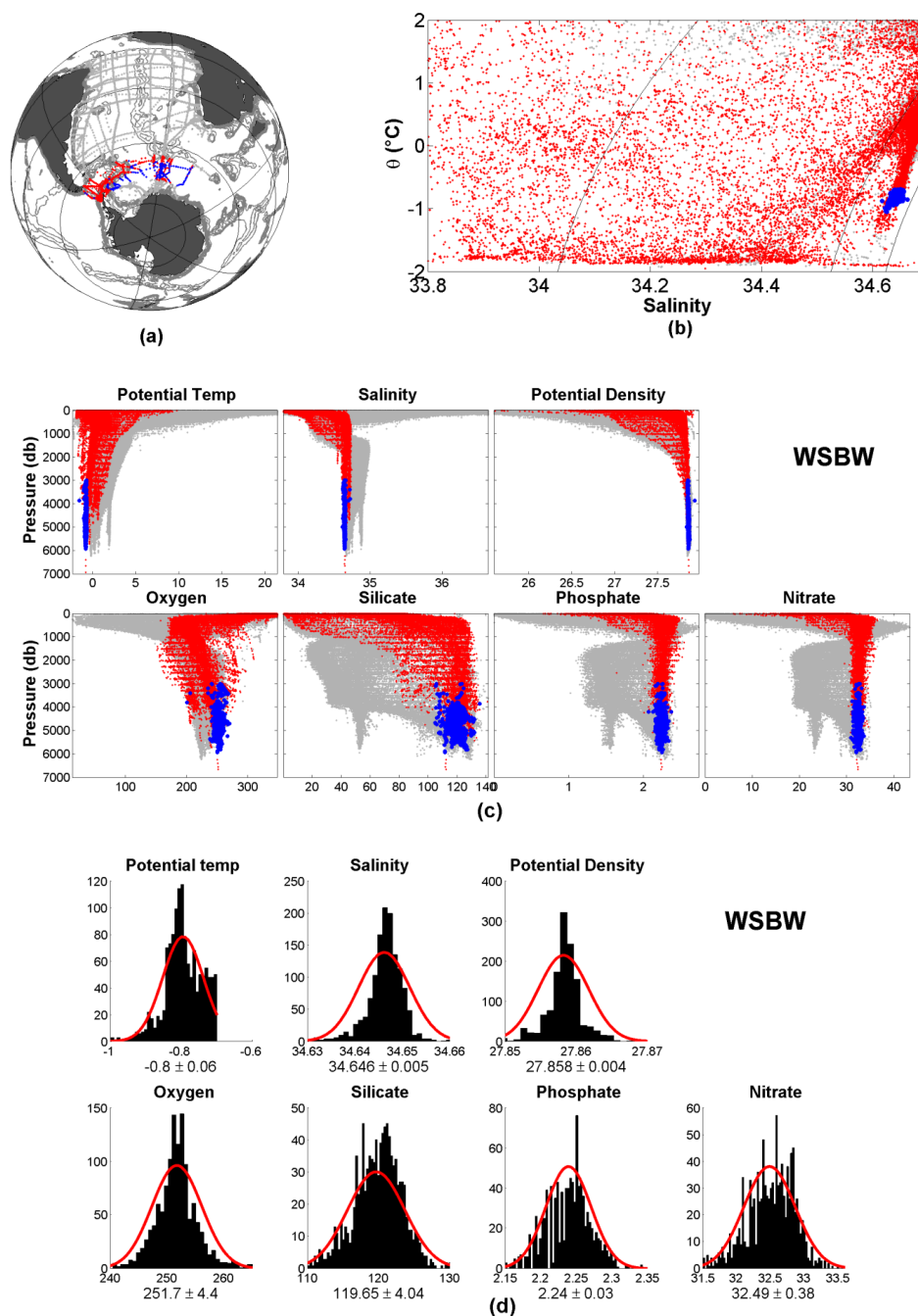


Figure 21: Overview of Weddell Sea Bottom Water (WSBW):

Panel a) shows the formation area used to define the water mass, panel b) show a T-S diagram and panel c) the distribution of key properties vs. pressure. In panel d) we show bar plots of the data distribution of samples used to define the water mass. Potential Temperature in ( $^{\circ}\text{C}$ ), Potential Density in  $\text{kg}/\text{m}^3$ , Oxygen and nutrients in  $\mu\text{mol}/\text{kg}^3$ . The red Gaussian fit shows mean and  $\sigma$  based on selected data.



643

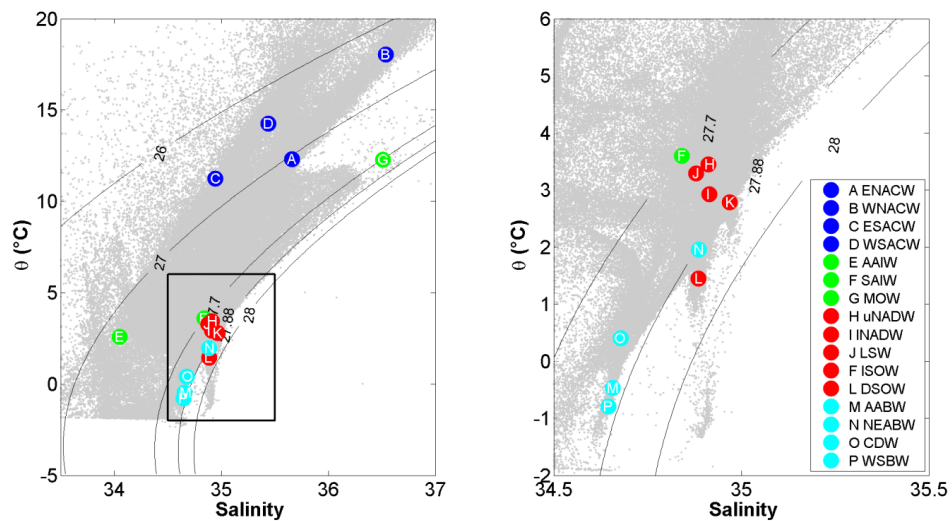


Figure 22: Potential temperature / Salinity distribution of the 16 main SWTs in the Atlantic Ocean discussed in this study. Colored dots with letters A-P show the mean value of each SWT and gray dots show all the data from GLODAPv2.

644



645

646

647

648

Table 1: Table of all the water masses and the four main layers as defined in this study.  
The variables defined are used to select water samples that defines water masses in the formation regions.

Layer	SWT	Longitude	Latitude	Pressure dbar	Potential Temperature °C	Salinity	Potential Density kg m <sup>-3</sup>	Oxygen μmol kg <sup>-1</sup>	Silicate μmol kg <sup>-1</sup>
Upper Layer	ENACW	15°W–25°W	39°N–48°N	100–500	---	---	26.50–27.30	---	---
	WNACW	50°W–70°W	24°N–37°N	100–1000	---	---	26.30–26.60	---	< 3
	WSACW	25°W–60°W	30°S–45°S	100–1000	---	> 34.5	26.00–27.00	< 230	< 5
	ESACW	0–15°E	30°S–40°S	200–700	---	---	26.00–27.20	200–240	< 10
Intermediate Layer	AAIW	25°W–55°W	45°S–60°S	> 300	> -0.5	---	26.95–27.50	> 230	< 30
	SAIW	35°W–55°W	50°N–60°N	100–500	> 4.5	< 34.6	> 27.65	---	---
	MOW	6°W–24°W	33°N–48°N	> 300	---	36.35–36.65	---	---	---
Deep and Overflow Layer	uNADW	32°W–50°W	40°N–50°N	1200–2000	---	---	27.72–27.82	---	---
	INADW	32°W–50°W	40°N–50°N	2000–3000	---	---	27.76–27.88	---	---
	LSW	24°W–60°W	48°N–66°N	500–2000	---	---	27.68–27.88	---	---
	ISOW	0–45°W	50°N–66°N	1500–3000	---	> 34.95	> 27.83	---	---
	DSOW	19°W–46°W	55°N–66°N	> 1500	---	---	> 27.88	---	< 11
Bottom Layer	AABW	---	> 63°S	---	---	---	> 28.27	---	> 120
	CDW	< 60°W	55°S–65°S	200–1000	0–1	> 34.64	> 27.80	---	---
	WSBW	---	55°S–65°S	3000–6000	< -0.7	---	---	---	> 105
	NEABW	10°W–45°W	0–30°N	> 4000	> 1.8	---	---	---	---

649

650

651



**Table 2: The full name of the water masses discussed in this study, and the abbreviation.**

<b>Full name of Water Mass</b>	<b>Abbreviation</b>
East North Atlantic Central Water	ENACW
West North Atlantic Central Water	WNACW
West South Atlantic Central Water	WSACW
East South Atlantic Central Water	ESACW
Antarctic Intermediate Water	AAIW
Subarctic Intermediate Water	SAIW
Mediterranean Overflow Water	MOW
Upper North Atlantic Deep Water	uNADW
Lower North Atlantic Deep Water	INADW
Labrador Sea Water	LSW
Iceland-Scotland Overflow Water	ISOW
Denmark Strait Overflow Water	DSOW
Antarctic Bottom Water	AABW
Circumpolar Deep Water	CDW
Weddell Sea Bottom Water	WSBW
Northeast Atlantic Bottom Water	NEABW



Table 3: Table of the mean value, and the standard deviation, of all variables for all the water masses discussed in this study.

Layer	SWTs	Potential Temperature (°C)	Salinity	Potential Density (kg m <sup>-3</sup> )	Oxygen (μmol kg <sup>-1</sup> )	Silicate (μmol kg <sup>-1</sup> )	Phosphate (μmol kg <sup>-1</sup> )	Nitrate (μmol kg <sup>-1</sup> )
Upper Layer	ENACW	12.31±0.95	35.662±0.124	27.039±0.097	234.4±13.2	3.67±1.20	0.57±0.16	9.34±2.38
	WNACW	18.03±0.47	36.536±0.079	26.441±0.069	204.3±9.3	1.32±0.46	0.17±0.06	3.68±1.16
	ESACW	11.26±2.25	34.944±0.272	26.659±0.207	219.2±9.1	5.50±1.96	0.96±0.31	13.27±4.73
	WSACW	14.27±2.02	35.439±0.320	26.451±0.191	216.0±6.2	2.60±0.99	0.56±0.24	6.85±3.60
Intermediate Layer	AAIW	2.58±0.56	34.051±0.135	27.148±0.125	303.2±28.1	15.68±6.78	1.79±0.23	24.65±2.95
	SAIW	3.60±0.41	34.841±0.043	27.700±0.025	294.9±8.9	8.57±0.74	1.04±0.06	15.69±0.86
	MOW	12.28±0.77	36.510±0.081	27.704±0.150	186.3±10.7	7.22±1.75	0.74±0.11	12.61±1.96
	uNADW	3.45±0.43	34.913±0.039	27.772±0.018	276.7±10.9	11.39±0.78	1.11±0.05	17.10±0.55
Deep and Overflow Layer	uNADW	2.93±0.25	34.914±0.018	27.823±0.025	278.2±4.6	13.21±1.44	1.10±0.05	16.77±0.50
	LSW	3.29±0.39	34.880±0.033	27.760±0.034	286.8±9.1	9.77±0.86	1.08±0.06	16.32±0.60
	ISOW	2.78±0.24	34.968±0.011	27.880±0.024	274.5±4.0	13.73±2.66	1.09±0.06	16.21±0.67
	DSOW	1.45±0.38	34.886±0.016	27.922±0.025	298.2±5.1	8.95±0.88	0.97±0.06	14.18±0.62
	AABW	-0.47±0.23	34.657±0.007	27.853±0.005	238.6±9.8	124.91±2.33	2.27±0.03	32.83±0.45
	CDW	0.40±0.22	34.678±0.012	27.824±0.010	204.2±10.2	115.18±7.99	2.31±0.06	33.42±0.93
Bottom Layer	WSBW	-0.80±0.06	34.646±0.005	27.858±0.004	251.7±4.4	119.65±4.04	2.24±0.03	32.49±0.38
	NEABW	1.95±0.06	34.887±0.008	27.885±0.003	245.8±3.7	47.07±2.33	1.49±0.04	22.27±0.53